FINAL PROJECT – MN 234876

ANALYSIS OF POLYURETHANE FOAM STRENGTH ON FIBER-BASED VESSELS

Gilang Gemilang Wahyu Wahab
NRP 5018221109 / ID 253157

Supervising Lecturer

Prof. Chang Yong Song

Dr. Eng. Ir. Septia Hardy Sujiatanti, S.T., M.T.

NAVAL ARCHITECTURE AND MARINE ENGINEERING STUDY PROGRAM
DEPARTMENT OF NAVAL ARCHITECTURE
FACULTY OF MARINE TECHNOLOGY
SEPULUH NOPEMBER INSTITUTE OF TECHNOLOGY
MOKPO NATIONAL UNIVERSITY
MOKPO
2026

This page has been intentionally left blank.

TUGAS AKHIR – MN 234876

ANALISIS KEKUATAN BUSA POLIURETAN KAKU PADA KAPAL BERBAHAN FIBER

Gilang Gemilang Wahyu Wahab

NRP 5018221109 / ID 253157

Dosen Pembimbing

Prof. Chang Yong Song

Dr. Eng. Ir. Septia Hardy Sujiatanti, S.T., M.T.

NAVAL ARCHITECTURE AND MARINE ENGINEERING STUDY PROGRAM

DEPARTEMEN TEKNIK PERKAPALAN

FAKULTAS TEKNOLOGI KELAUTAN

INSTITUT TEKNOLOGI SEPULUH NOPEMBER

MOKPO NATIONAL UNIVERSITY

MOKPO

2026

Halaman ini sengaja dikosongkan.

FINAL PROJECT – MN 234876

ANALYSIS OF POLYURETHANE FOAM STRENGTH ON FIBER-BASED VESSELS

Gilang Gemilang Wahyu Wahab

NRP 5018221109 / ID 253157

A thesis submitted in fulfilment of the requirements for the award of the degree of Bachelor of Engineering

(Naval Architecture)

Supervising Lecturer

Prof. Chang Yong Song

Dr. Eng. Ir. Septia Hardy Sujiatanti, S.T., M.T.

NAVAL ARCHITECTURE AND MARINE ENGINEERING STUDY PROGRAM

DEPARTMENT OF NAVAL ARCHITECTURE

FACULTY OF MARINE TECHNOLOGY

SEPULUH NOPEMBER INSTITUTE OF TECHNOLOGY

MOKPO NATIONAL UNIVERSITY

MOKPO

2026

This page has been intentionally left blank.

LEMBAR PENGESAHAN

ANALISIS KEKUATAN BUSA POLIURETAN KAKU PADA KAPAL BERBAHAN FIBER

TUGAS AKHIR

Diajukan untuk Memenuhi Salah Satu Syarat
Memperoleh Gelar Sarjana Teknik
pada
Program Sarjana Departemen Teknik Perkapalan
Fakultas Teknologi Kelautan
Institut Teknologi Sepuluh Nopember

Oleh:
GILANG GEMILANG WAHYU WAHAB
NRP 5018221109

Disetujui oleh:

Dosen Pembimbing II	Dosen Pembimbing I
Dr. Eng. Ir. Septia Hardy Sujiatanti, S.T., M.T.	Prof. Chang Yong Song
NIP 198409212012122001	

Mengetahui,
Kepala Departemen Naval Architecture and Ocean Engineering

Professor Choi Jung-Kyu

MOKPO, 11 Juni 2026

Halaman ini sengaja dikosongkan.

APPROVAL SHEET

ANALYSIS OF POLYURETHANE FOAM STRENGTH ON FIBER-BASED VESSELS

FINAL PROJECT

Submitted to Fulfill One of the Requirements
Obtaining a Bachelor of Engineering Degree
on
Undergraduate Program of Department of Naval Architecture
Faculty of Marine Technology
Sepuluh Nopember Institute of Technology

By:
GILANG GEMILANG WAHYU WAHAB
NRP 5018221109

Approved by:

Supervisor II

Dr. Eng. Ir. Septia Hardy Sujiatanti, S.T., M.T.
NIP 198409212012122001

Supervisor I

Prof. Chang Yong Song

Acknowledge by,
Head of Department of Naval Architecture and Ocean Engineering

Professor Choi Jung-Kyu

MOKPO, 11 JUNE 2026

This page has been intentionally left blank.

PERNYATAAN ORISINALITAS

Yang bertanda tangan di bawah ini:

Nama mahasiswa / NRP	: Gilang Gemilang Wahyu Wahab / 5018221109
Program studi	: Teknik Perkapalan FTK ITS
Dosen Pembimbing	: Prof. Chang Yong Song
Dosen Pembimbing / NIP	: Dr. Eng. Ir. Septia Hardy Sujiatanti, S.T., M.T. /

198409212012122001

Dengan ini menyatakan bahwa Tugas Akhir dengan judul "ANALISIS KEKUATAN BUSA POLIURETAN KAKU PADA KAPAL BERBAHAN FIBER" adalah hasil karya sendiri, bersifat orisinal, dan ditulis dengan mengikuti kaidah penulisan ilmiah.

Bilamana di kemudian hari ditemukan ketidaksesuaian dengan pernyataan ini, maka saya bersedia menerima sanksi sesuai dengan ketentuan yang berlaku di Institut Teknologi Sepuluh Nopember.

Mokpo, 11 Juni 2026
Mahasiswa

Gilang Gemilang Wahyu Wahab
NRP 5018221109 / 253157

Mengetahui 2
Dosen Pembimbing

Dr. Eng. Ir. Septia Hardy Sujiatanti, S.T., M.T.
NIP 198409212012122001

Mengetahui 1
Dosen Pembimbing

Prof. Chang Yong Song

This page has been intentionally left blank.

STATEMENT OF ORIGINALITY

The undersigned below:

Name of student / NRP : Gilang Gemilang Wahyu Wahab / 5018221109
Department : Department of Naval Architecture Faculty of Marine Technology ITS
Advisor 1 : Prof. Chang Yong Song
Advisor 2 / NIP : Dr. Eng. Ir. Septia Hardy Sujiatanti, S.T., M.T. / 198409212012122001

Hereby declare that the final project with the title of “ANALYSIS OF POLYURETHANE FOAM STRENGTH ON FIBER-BASED VESSELS” is the result of my own work, is original, and is written by following the rules of scientific writing.

If in the future there is a discrepancy with this statement, then I am willing to accept sanctions in accordance with the provisions that apply at Institut Teknologi Sepuluh Nopember.

Mokpo, June 11, 2026
Student

Gilang Gemilang Wahyu Wahab
NRP 5018221109 / 253157

Acknowledge by,
Supervising Lecturer 2

Dr. Eng. Ir. Septia Hardy Sujiatanti, S.T., M.T.
NIP 198409212012122001

Acknowledge by,
Supervising Lecturer 1

Prof. Chang Yong Song

This page has been intentionally left blank.

REVISION SHEET

ANALYSIS OF POLYURETHANE FOAM STRENGTH ON FIBER-BASED VESSELS

FINAL PROJECT

Revised according to the results of the Final Assignment Exam
Date June 12, 2026
Undergraduate Program of Department of Naval Architecture
Faculty of Marine Technology
Sepuluh Nopember Institute of Technology

By:
GILANG GEMILANG WAHYU WAHAB
NRP 5018221109

Approved by the Final Project Exam Examiner Team:

Sol Ha

1. Prof. Sol-Ha

Choi

2. Prof. Choi Jung-Kyu

Approved by the Final Project Supervisor:

1. Prof. Chang Yong Song
2. Dr. Eng. Ir. Septia Hardy Sujiatanti, S.T., M.T. ………………

MOKPO, 11 JULY 2026

This page has been intentionally left blank.

PAGE OF ALLOCATION

Dedicated to my parents for all their support and prayers.

This page has been intentionally left blank.

FOREWORD

Praise be to God Almighty, for it is by His grace and guidance that this work has been successfully completed. This document is the result of a long process of learning, analysis, and reflection, shaped by the knowledge and experience gained throughout my academic and professional journey.

I would also like to extend my sincere appreciation to the following individuals and institutions who have supported and assisted me throughout the process:

1. Prof. Chang Yong Song, as the Supervising Lecturer, for his guidance and motivation throughout the process and preparation of this Final Project;
2. Prof. Sol-Ha and Prof. Choi Jung-Kyu, as the examiners of this Final Project.;
3. Ir. Teguh Putranto, S.T., M.T., Ph.D., as the Head of the Department of Naval Architecture, Faculty of Marine Technology, ITS;
4. Dr. Eng. Ir. Septia Hardy Sujiatanti, S.T., M.T., as the Author's Academic Advisor, for his continuous support and motivation during the course of study;
5. Friends of the ITS-MNU Joint Degree Program Batch 5, for their mutual support in completing this Final Project.
6. The Author's beloved family, for their endless prayers, encouragement, and motivation;
7. Friends from P-62, for their constant support from Indonesia;
8. And all other individuals who have contributed to the completion of this Final Project and whose names cannot be mentioned one by one;

The Author is fully aware that this Final Project is still far from perfect, and therefore constructive criticism and suggestions are highly appreciated. Finally, it is hoped that this report will be beneficial to many parties.

Mokpo, 18th June 2026

Gilang Gemilang Wahyu Wahab

This page has been intentionally left blank.

ANALISIS KEKUATAN BUSA POLIURETAN KAKU PADA KAPAL BERBAHAN FIBER

Nama Mahasiswa	: Gilang Gemilang Wahyu Wahab
NRP	: 5018221109 / 253157
Departemen / Fakultas	: Teknik Perkapalan / Teknologi Kelautan
Dosen Pembimbing	: 1. Prof. Chang Yong Song
	2. Dr. Eng. Ir. Septia Hardy Sujiatanti, S.T., M.T.

ABSTRAK

Busa poliuretan kaku sel tertutup (RPUF) banyak digunakan pada kapal berbahan komposit fiber sebagai inti sandwich, daya apung cadangan, dan insulasi, sehingga kekuatan tekannya menentukan kemampuan strukturalnya. Penelitian ini mengevaluasi, dengan metode elemen hingga (ANSYS), kekuatan tekan RPUF sebagai fungsi densitas (40–120 kg/m³) dan arah pengembangan busa, dibandingkan terhadap ASTM D1621, kemudian menerapkan busa yang telah tervalidasi sebagai inti panel sandwich fiberglass. Pada fase kupon, sepuluh analisis menunjukkan tegangan tekan meningkat mengikuti $\sigma \propto \rho^2$, sekitar 31% lebih tinggi sejajar arah pengembangan, dan sesuai data publikasi dalam ±3% pada densitas rendah. Pada fase struktural, panel sandwich 1 m × 1 m (kulit 3 mm / inti 20 mm / kulit 3 mm) dibebani tekanan lateral, geser bidang, dan tekuk. Dibandingkan laminat kulit tunggal setara, inti busa mengurangi defleksi sekitar 26 kali, menurunkan tegangan kulit puncak sekitar 7 kali, dan menaikkan ketahanan tekuk sekitar 25 kali dengan tambahan berat hanya 15%.

Kata kunci: busa poliuretan kaku, kekuatan tekan, struktur sandwich, fiberglass, analisis elemen hingga.

Halaman ini sengaja dikosongkan.

ANALISIS KEKUATAN BUSA POLIURETAN KAKU PADA KAPAL BERBAHAN FIBER

Nama Mahasiswa	: Gilang Gemilang Wahyu Wahab
NRP	: 5018221109 / 253157
Departemen / Fakultas	: Teknik Perkapalan / Teknologi Kelautan
Dosen Pembimbing	: 1. Prof. Chang Yong Song
	2. Dr. Eng. Ir. Septia Hardy Sujiatanti, S.T., M.T.

ABSTRACT

Rigid closed-cell polyurethane foam (RPUF) is widely used in fiber-reinforced plastic vessels as a sandwich core, reserve buoyancy, and insulation, where its compressive strength governs its structural duty. This study evaluates, by finite element analysis in ANSYS, the compressive strength of RPUF as a function of density (40–120 kg/m^3) and rise direction, benchmarked against ASTM D1621, and then applies the validated foam as the core of a representative fiberglass sandwich hull panel. In the coupon phase, ten analyses show that compressive stress rises with density following $\sigma \propto \rho^2$, is about 31% higher parallel to the rise direction, and agrees with published data to within about 3% at low density, over-predicting at high density because the linear-elastic model has no yield plateau. The coupon quantity is the compressive stress at 2% strain (modulus-controlled, $\sigma \propto \rho^2$), not the true compressive strength; Phase 1 characterises stiffness-controlled stress rather than predicting strength. In the structural phase, a 1 m × 1 m sandwich panel (3 mm skin / 20 mm core / 3 mm skin) is loaded under lateral pressure, in-plane shear, and buckling. Against an equal-skin single-skin laminate the foam core reduces deflection about 26 times, lowers peak skin stress about 7 times, and raises buckling resistance about 25 times for only 15% more weight. The results quantify both the material behaviour of RPUF and the structural benefit it delivers as a fiberglass sandwich core.

Keywords: rigid polyurethane foam, compressive strength, sandwich structure, fiberglass, finite element analysis.

This page has been intentionally left blank.

LIST OF CONTENTS

LIST OF FIGURES

LIST OF TABLES

This page has been intentionally left blank.

LIST OF SYMBOLS

σ	=	Normal (compressive) stress
$\sigma_{\parallel}$, $\sigma_{\perp}$	=	Stress parallel / perpendicular to rise direction
ε	=	Strain
E, Ex, Ey, Ez	=	Elastic moduli (orthotropic)
ν	=	Poisson's ratio
G, Gxy, Gyz, Gxz	=	Shear moduli
ρ, ρ*, ρs	=	Density; foam and solid-polymer density
D	=	Sandwich flexural rigidity
S	=	Sandwich transverse-shear rigidity
tf, tc	=	Face (skin) and core thickness
d	=	Distance between face centroids
q	=	Lateral pressure
a	=	Panel side length
w	=	Out-of-plane deflection
M, V	=	Bending moment and shear force per unit width
λ, Pcr	=	Buckling load multiplier; critical buckling load
[K], {u}, {F}	=	Stiffness matrix, nodal displacement and load vectors

This page has been intentionally left blank.

CHAPTER 1
INTRODUCTION

1.1 Background

Fiber-reinforced plastic (FRP) vessels are now standard in small and medium craft for their high strength-to-weight ratio, corrosion resistance, and formability. Within these hulls, rigid closed-cell polyurethane foam (RPUF) serves as the lightweight core of sandwich laminates, as reserve buoyancy, and as thermal insulation. In each of these roles the foam carries or transfers compressive load, so its compressive strength is the property that governs how much structural duty it can take.

The compressive strength of RPUF is set primarily by density: denser foam has thicker, stiffer cell walls and resists compression more strongly, with mechanical properties rising steeply and monotonically across the producible range. The foam is also anisotropic, because its cells elongate along the direction in which the foam rises during curing, so stiffness and strength differ parallel versus perpendicular to that rise direction. A complete characterization therefore treats density and loading direction together.

Compressive strength is measured under a standardized test, ASTM D1621 for rigid cellular plastics, which fixes specimen geometry and loading so that results are comparable between materials and studies. FEM reproduces this test numerically, which makes it possible to evaluate compressive behavior across several producible densities, and in loading directions that are awkward to test physically, without fabricating a specimen for every case.

Despite the wide use of RPUF in fiber-based vessels, finite-element-based compressive characterization across the full range of producible densities, with material anisotropy explicitly modeled and the results benchmarked against the standard test, remains limited. This study addresses that gap by building a solid-element model of the standard compression specimen, applying it to five producible densities, and then placing the validated foam between fiberglass skins as a representative hull panel to quantify the structural benefit it delivers.

1.2 Problem Formulation

Based on the background above, the following research questions are addressed:

1. How do the compressive stress at 2% strain of RPUF, its anisotropy (loading parallel versus perpendicular to the rise direction), and its stress-density scaling behave across the producible density range (40–120 kg/m³)?
2. To what extent does a rigid polyurethane foam core enhance the structural performance of a fiber-based hull panel (deflection, skin stress, and buckling) compared with an equivalent single-skin laminate, and how does the foam-cored sandwich panel respond to lateral design pressure and in-plane shear?
3. Is partial substitution of solid laminate by a foam-cored sandwich panel cost-effective?

1.3 Objectives

The objectives of this research are:

1. Quantify the relationship between RPUF density and its compressive stress at 2% strain across the producible range.
2. Quantify the effect of material anisotropy, namely the rise-direction dependence, on the compressive stress at 2% strain.
3. Characterize the compressive stress at 2% strain as a function of density, and benchmark the results against ASTM D1621 and published data.
4. Quantify the structural enhancement provided by a rigid polyurethane foam core in a representative sandwich hull panel, covering deflection, skin stress, and buckling, and assess the cost-effectiveness of partial foam substitution.

1.4 Constraints

The constraints of the problem are as follows:

1. Analysis covers rigid closed-cell polyurethane foam at five producible densities (40, 60, 80, 100, and 120 kg/m³).
2. The analysis is performed by the finite element method in ANSYS using a solid-element model of the ASTM D1621 compression specimen (equivalent to ISO 844 and EN 826).
3. The foam is modeled as orthotropic (transversely isotropic). The work is carried out in two phases: a coupon-level uniaxial compression study (Phase 1) and a sandwich-

panel structural study (Phase 2) that applies the validated foam as a hull-panel core under lateral pressure, in-plane shear, and buckling.

4. The work spans the coupon (material) level and a representative midship sandwich panel; full-vessel structural modeling and sea-keeping loads are outside this scope. The sandwich design basis follows ISO 12215-5.

1.5 Benefits

The benefits of this research are as follows:

1. Academically, it supports knowledge development in marine composite materials and provides baseline data for foam material selection in vessel applications.
2. Practically, it provides evidence-based guidance for shipyards and marine engineers implementing polyurethane foam solutions for improved vessel performance and cost optimization.
3. Industrially, identifying cost-effective foam substitution strategies can reduce construction cost while maintaining structural integrity and safety.

1.6 Hypothesis

Compressive strength is expected to increase monotonically with density following a power-law relationship, and to be higher parallel to the foam rise direction than perpendicular to it. The finite element results should agree closely with standard analytical and experimental references at low density; any divergence at higher density is attributed to the limits of the linear-elastic assumption, which a crushable-foam model would resolve. At the structural level, the foam-cored sandwich panel is expected to be far stiffer and stronger than an equal-skin single-skin laminate, so that a small core mass produces a large reduction in deflection and skin stress and a large increase in buckling resistance.

This page has been intentionally left blank.

CHAPTER 2
LITERATURE STUDY

2.1 Basic Theory

The theoretical basis directly related to and used in this study is set out below.

2.1.1 Concept and Marine Applications of Sandwich Structures

A sandwich structure achieves maximum structural efficiency through optimized material distribution: two thin, strong face sheets are separated by a lightweight core. The face sheets, typically fiber-reinforced composites, carry the primary in-plane loads and bending moments, while the core maintains the separation between the faces and transfers the shear between them. This arrangement creates a structure whose performance far exceeds the sum of its parts, combining low weight, a high strength-to-weight ratio, and high specific energy absorption (Wang et al., 2024).

2.1.2 Finite Element Method

Finite elements are small interconnected units used to model a larger structure. The method models irregular geometries easily, handles common loading and boundary conditions, accommodates several different materials because element equations are evaluated individually, and allows element size to be refined where needed. It is a general numerical method for solving the differential equations of structural, thermal, and flow problems, and it lets engineers predict structural behavior before physical testing, reducing development cost (Belinha, 2024).

2.1.3 Fiberglass in Marine Construction

Fiber Reinforced Plastic (FRP) transformed marine construction by offering superior durability, reduced maintenance, and design flexibility compared with traditional wooden construction, which suffered from rot and marine-borer attack. Fiberglass is durable, lightweight, and easily formed to complex hull shapes, enabling vessels with enhanced performance at lower construction and maintenance cost over the service life (Febrian & Buwono, 2024).

2.1.4 Sandwich Construction in Fiberglass

Combining fiberglass face sheets with a lightweight core creates structures with optimal weight efficiency while maintaining rigidity and strength. The core reduces the overall specific gravity while the fiber-reinforced faces provide the strength, addressing the central marine-engineering challenge of achieving structural strength at minimum weight, which directly affects performance, fuel efficiency, and payload (Junaedi et al., 2023).

2.1.5 Polyurethane Foam

Rigid closed-cell polyurethane foam emerged as a core material that suits marine construction: low density to minimize weight, sufficient strength to transfer load between faces, and good resistance to the marine environment. Closed-cell formulations resist water absorption, maintain properties over long service, and add buoyancy and thermal insulation, while remaining cost-effective to manufacture and install (Quang et al., 2025).

2.1.6 Integration of Foam Cores and Fiberglass Faces

The face-to-core interface is a critical design consideration, since the bond must transfer load effectively while maintaining integrity under dynamic marine loading. Modern manufacturing, improved adhesives, and a better understanding of interface mechanics have made foam-cored fiberglass sandwich construction a viable option across recreational and commercial vessels (Mohd Radzi et al., 2022).

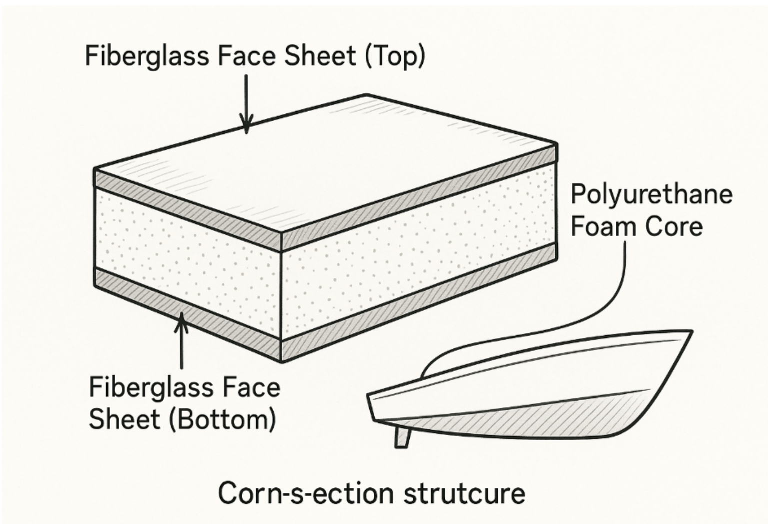

Figure 2.1 Cross-section of a fiberglass sandwich structure: fiberglass face sheets over a polyurethane foam core.

2.2 Governing Equations

The relationships below underpin the verification, the density characterization, and the sandwich-panel analysis. For a linear-elastic material under uniaxial stress, stress is proportional to strain through the elastic modulus (Hooke's law), Equation 2.1. This relation verifies the model, since at a prescribed strain the computed stress must equal the modulus times the strain (Logan, 2017).

$$\sigma = E\varepsilon \tag{2.1}$$

Where:

σ	=	stress
E	=	elastic modulus
ε	=	strain

For cellular solids the relative stiffness and strength scale with relative density through the Gibson–Ashby relations, Equation 2.2; the asterisk denotes the foam and the subscript s the solid polymer (Gibson & Ashby, 1997).

$$\frac{E^*}{E_s} = C_1\left(\frac{\rho^*}{\rho_s}\right)^2 \frac{\sigma^*}{\sigma_s} = C_2\left(\frac{\rho^*}{\rho_s}\right)^{3/2} \tag{2.2}$$

Where:

E*, σ*	=	foam modulus and strength
Es, σs	=	solid-polymer modulus and strength
ρ*, ρs	=	foam and solid-polymer density
C1, C2	=	cell-geometry constants

Because the foam is transversely isotropic, the through-thickness normal strain depends on all three normal stresses through the orthotropic compliance, Equation 2.3, the constitutive law assigned to the foam in ANSYS.

$$\varepsilon_z = \frac{\sigma_z}{E_z} - \nu_{xz}\frac{\sigma_x}{E_x} - \nu_{yz}\frac{\sigma_y}{E_y} \tag{2.3}$$

Where:

εz	=	through-thickness strain
σx, σy, σz	=	normal stresses
Ex, Ey, Ez	=	elastic moduli
νxz, νyz	=	Poisson’s ratios

For a sandwich with thin faces of thickness tf separated by a core of thickness tc, the flexural rigidity per unit width is dominated by the membrane action of the faces about the mid-plane, Equation 2.4 (Allen, 1969).

$$D = \frac{E_f t_f d^2}{2} + \frac{E_f t_f^3}{6} + \frac{E_c t_c^3}{12} \tag{2.4}$$

Where:

D	=	flexural rigidity per unit width
Ef, Ec	=	face and core modulus
tf, tc	=	face and core thickness
d	=	distance between face centroids

The transverse-shear rigidity of the sandwich is carried almost entirely by the core, Equation 2.5 (Allen, 1969).

$$S = \frac{G_c d^2}{t_c} \tag{2.5}$$

Where:

S	=	transverse-shear rigidity
Gc	=	core shear modulus
d	=	distance between face centroids
tc	=	core thickness

Under uniform lateral pressure q, a simply-supported square plate of side a deflects by a bending term plus a shear term, Equation 2.6; the shear term is significant because the core is soft (Timoshenko & Woinowsky-Krieger, 1959; Allen, 1969).

$$w_{max}=\alpha\frac{qa^4}{D}+\beta\frac{qa^2}{S} \tag{2.6}$$

Where:

wmax	=	maximum deflection
q	=	lateral pressure
a	=	panel side length
D	=	flexural rigidity
S	=	transverse-shear rigidity
α, β	=	plate coefficients

In a sandwich the bending moment is carried as a force couple in the faces and the shear force by the core, giving the face stress and core transverse shear of Equation 2.7 (Allen, 1969).

$$\sigma_f=\frac{M}{t_f d}\tau_c=\frac{V}{d} \tag{2.7}$$

Where:

σf	=	face stress
τc	=	core transverse shear
M	=	bending moment per unit width
V	=	shear force per unit width
tf	=	face thickness
d	=	distance between face centroids

Linear (eigenvalue) buckling solves the generalized eigenproblem of Equation 2.8 for the load multipliers; the critical buckling load is the first multiplier times the applied reference load.

$$([K]+\lambda_i[K_G])\{\phi_i\}=0P_{cr}=\lambda_1 P_{ref} \tag{2.8}$$

Where:

[K]	=	elastic stiffness matrix
[KG]	=	geometric stiffness matrix
λi	=	load multiplier (eigenvalue)
φi	=	buckling mode shape
Pcr	=	critical buckling load
Pref	=	applied reference load

The hydrostatic component of the design pressure follows Equation 2.9; the governing bottom-panel design pressure is obtained from ISO 12215-5, which adds slamming and area/location factors (ISO, 2019).

$$P_h = \rho_{sw} g h \tag{2.9}$$

Where:

P_h	=	hydrostatic pressure
ρ_{sw}	=	seawater density
g	=	gravitational acceleration
h	=	local head

The finite element method reduces structural equilibrium to the linear system of Equation 2.10 (Logan, 2017).

$$[K]\{u\} = \{F\} \tag{2.10}$$

Where:

[K]	=	global stiffness matrix
{u}	=	nodal displacement vector
{F}	=	applied load vector

2.3 Literature Review

Several previous studies are reviewed below as comparison material.

Rathika et al. (2024), "The Effect of Damages on Modal Frequencies of Flat Glass Fiber Reinforced Polyurethane Foam Sandwich Structures," applied the finite element method to glass-fiber/polyurethane foam panels and showed that modal frequencies decrease with damage. It shares the present use of FEA on polyurethane foam systems but addresses modal and damage behavior rather than density-dependent compressive strength.

Junaedi, Khan, and Sebaey (2023), "Characteristics of Carbon-Fiber-Reinforced Polymer Face Sheet and Glass-Fiber-Reinforced Rigid Polyurethane Foam Sandwich Structures under Flexural and Compression Tests," measured the response of RPUF-core sandwich panels under flexure and compression. It is closely related, since it tests RPUF under compression, but focuses on the composite panel and faces, whereas the present study isolates the foam core and its density dependence.

Kim et al. (2019), "Effect of Repetitive Impacts on the Mechanical Behavior of Glass Fiber-reinforced Polyurethane Foam," showed that the compressive strength and modulus of RPUF are reduced by repetitive impact. It relates through its focus on RPUF compressive properties and anisotropy, but addresses impact durability for cryogenic storage rather than quasi-static density-dependent strength.

Eashwar Raaj et al. (2024) reported mechanical improvements from hybrid fiber reinforcement of a polyurethane core. It relates through the polyurethane-core sandwich theme but emphasizes natural-fiber hybridization and free-vibration behavior rather than the compressive strength of the foam itself.

A study in Jurnal Jaring SainTek (2022) examined the impact strength of fiberglass and polyurethane foam sandwich laminates at different polyol-to-isocyanate ratios. It relates through its fiberglass-and-foam subject but tests impact resistance of the laminate rather than density-dependent compressive strength.

Boesono, Saraswati, and Setiyanto (2018) quantified the polyurethane foam required for reserve buoyancy in a 5 GT fiber fishing vessel. It establishes the marine application that motivates the present work but addresses buoyancy quantity rather than compressive strength, and uses no finite element analysis.

CHAPTER 3
RESEARCH METHODOLOGY

3.1 Flowchart

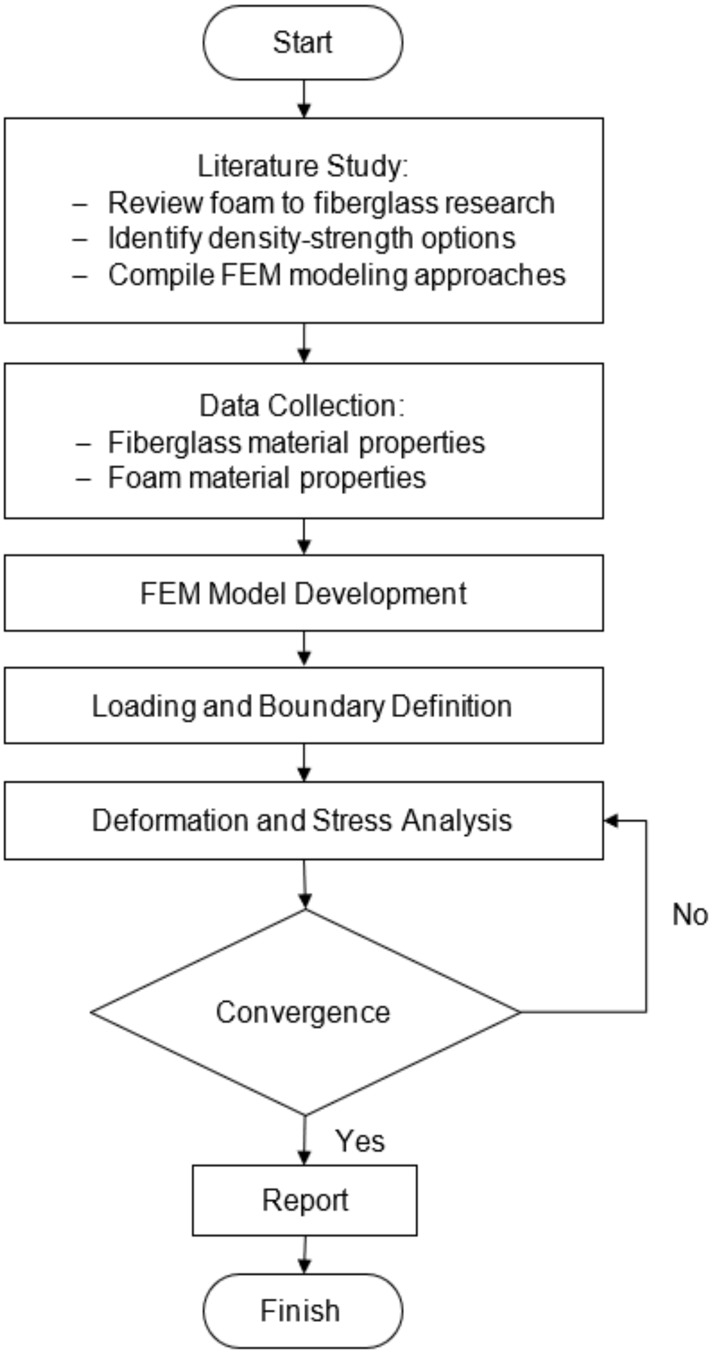

Figure 3.1 Flowchart of the research method.

3.2 Working Stages

The work was structured through the following stages.

3.2.1 Literature Study

A literature study was conducted to gather existing knowledge on the compressive behavior of rigid polyurethane foam, the dependence of its properties on density, foam anisotropy, and finite element methods for cellular materials. Standard test methods for the compression of rigid cellular plastics were reviewed to establish the basis for the model.

The literature study covered four areas. First, the mechanics of cellular solids were reviewed, in particular the Gibson–Ashby framework that relates the stiffness and strength of a foam to its relative density through power laws; this framework provides the theoretical basis for the density-dependent material constants used later in the model. Second, the anisotropy of rigid polyurethane foam was examined, since the cells elongate along the foam rise direction during curing and give the material a transversely isotropic response, stiffer parallel to the rise direction than perpendicular to it. Third, the finite element method for solid continua was reviewed, together with the element formulations and mesh requirements appropriate to a compressive stress field. Fourth, the relevant test and design standards were collected: ASTM D1621, with its equivalents ISO 844 and EN 826, for the compression of rigid cellular plastics, and ISO 12215-5 for the scantling and design-pressure basis of small-craft sandwich hulls used in Phase 2.

3.2.2 Data Collection (Phase 1)

The density-dependent orthotropic elastic constants of closed-cell rigid polyurethane foam were assembled across the producible range of 40 to 120 kg/m³, together with the specimen geometry defined by ASTM D1621. The constants, derived from the Gibson–Ashby density relation and calibrated to Shivakumar & Deb (2022) and Hamilton et al. (2013), are listed in Table 3.1. The foam rise direction is taken as the material Z axis, so that the through-thickness properties differ from the in-plane properties, as illustrated in Figure 3.3.

The producible density range of 40 to 120 kg/m³ was selected because it spans the grades commonly used for marine sandwich cores, reserve buoyancy, and insulation, from light insulating foam at the lower bound to structural-grade foam at the upper bound. The orthotropic elastic constants for each density were not measured directly but derived from the Gibson–Ashby relations, which state that the elastic modulus of a closed-cell foam scales with the square of its relative density, $E^*/E_s = C(\rho^*/\rho_s)^2$, where the asterisk denotes the foam and the subscript s the solid polymer. Taking the solid polyurethane as the base material and calibrating the proportionality constant to the experimental data of Shivakumar and Deb (2022) and the anisotropic measurements of Hamilton et al. (2013), the in-plane modulus Ex = Ey and the through-thickness modulus Ez were computed for each of the five densities and listed in Table 3.1.

Because the cells are elongated along the rise direction, the through-thickness modulus Ez is consistently higher than the in-plane modulus Ex = Ey; at 40 kg/m³ the two moduli are 8.5 MPa and 6.5 MPa respectively, and at 120 kg/m³ they rise to 76.0 MPa and 58.0 MPa. This directional difference, illustrated in Figure 3.3, is the physical source of the anisotropy quantified in Phase 1. The shear moduli Gxy and Gyz = Gxz and the Poisson's ratios were scaled consistently with the same relative-density law, and the rise direction was assigned to the material Z axis for every model so that the through-thickness properties are always those parallel to the rise. The values in Table 3.1 are the direct input to the material definition in ANSYS and should be confirmed against the datasheet of the specific foam grade before the results are treated as final.

ρ (kg/m³)	Ex = Ey (MPa)	Ez (MPa)	νxy	νyz = νxz	Gxy (MPa)	Gyz = Gxz (MPa)
40	6.5	8.5	0.32	0.3	2.46	3.2
60	14.5	19.0	0.32	0.3	5.49	7.15
80	26.0	34.0	0.31	0.3	9.92	12.85
100	41.0	53.5	0.3	0.3	15.77	20.36
120	58.0	76.0	0.3	0.3	22.31	28.84

Table 3.1 Orthotropic elastic properties of RPUF used in the model (Z = foam rise direction).

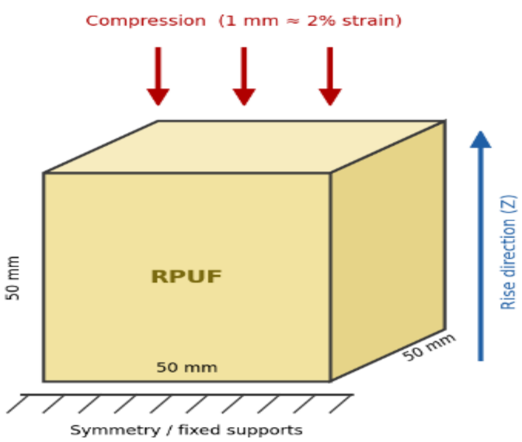

Figure 3.2 ASTM D1621 compression specimen modeled as a 50 mm solid cube.

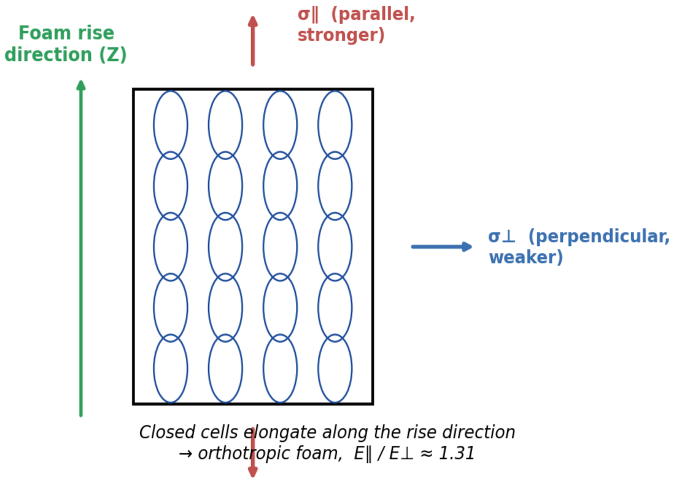

Figure 3.3 Foam cells elongate along the rise direction, making the foam orthotropic: stiffer and stronger parallel to rise (σ‖) than perpendicular (σ⊥).

3.2.3 Data Collection (Phase 2)

Phase 2 reuses the validated foam as the core of a three-layer fiberglass sandwich panel, so its input data set adds the skin material, the panel geometry, and the hull design loads to the foam database already assembled in Phase 1. The skins are a woven-roving E-glass/epoxy laminate represented as a homogenised orthotropic solid with an in-plane modulus of 16 GPa, a through-thickness modulus of 7 GPa, an in-plane shear modulus of 3.5 GPa, a transverse shear modulus of 2.6 GPa, an in-plane Poisson's ratio of 0.15, and a density of 1800 kg/m³; these constants are summarised in Table 3.2. The core is the 80 kg/m³ RPUF grade carried directly from Phase 1, retaining its orthotropic constants with the rise direction aligned to the panel through-thickness axis.

The panel represents a midship bottom plate spanning 1000 × 1000 mm between stiffeners, built from a 3 mm outer skin, a 20 mm foam core, and a 3 mm inner skin, for a total thickness of 26 mm. It is idealised as simply supported, with the through-thickness (Z) displacement restrained along the four bottom edges, in-plane motion left free, and one corner pinned to remove rigid-body movement. The governing lateral load follows ISO 12215-5:2019 for small-craft bottom panels; a representative design pressure of 50 kPa is applied to the outer skin for the analyses reported here and is to be replaced by the vessel-specific value once the craft parameters are fixed. Three load cases are collected: LC1 uniform lateral pressure, which produces skin bending stress and core transverse shear; LC2 in-plane edge shear for racking stiffness; and LC3 in-plane compression feeding an eigenvalue buckling solve. The core transverse shear strength, which bounds the core failure mode in LC1 and is not needed in Phase 1, is to be confirmed against the foam supplier datasheet for each density before the Phase 2 results are treated as final.

3.2.4 FEM Model Development

A three-dimensional solid model of the standard specimen was built in ANSYS Workbench (Static Structural). The mesh uses SOLID186 elements, twenty-node quadratic hexahedra suited to compressive stress fields, at a 2.5 mm element size, giving roughly 8,000 elements for the 50 mm cube. Because uniform uniaxial compression produces a spatially uniform stress field, the solution is mesh-independent for this homogeneous case, which a mesh-sensitivity check confirms.

The SOLID186 element was chosen because its quadratic (second-order) displacement interpolation represents the linear strain field of uniform compression exactly, so that even a coarse mesh reproduces the analytical stress without the artificial stiffening that can affect first-order elements. Each element is a twenty-node hexahedron with three translational degrees of freedom at every node, and the mesh was built as a structured, mapped grid of 2.5 mm cubes, giving twenty elements along each edge of the specimen and approximately 8,000 elements in total. A full integration scheme was used, which is appropriate for a bending-free compressive stress state.

A mesh-sensitivity study confirmed that this discretisation is adequate. The compressive stress of the 80 kg/m³ grade was recomputed for element sizes of 5.0, 2.5, and 1.25 mm, corresponding to roughly 1,000, 8,000, and 64,000 elements, and the result changed by less than 0.01% between the coarsest and the finest mesh, as summarised in Table 3.3. This near-perfect mesh independence is expected, because the uniform uniaxial compression of a homogeneous cube produces a spatially uniform stress field that any conforming mesh resolves exactly. The 2.5 mm element size was retained as a balance between resolution and solution time. The foam was assigned a linear orthotropic (transversely isotropic) constitutive law, in which the through-thickness normal strain depends on all three normal stresses through the orthotropic compliance matrix defined by the nine constants of Table 3.1; no plasticity or crushable-foam behaviour was included, so the model is valid only up to the onset of foam yield.

Table 3.3 Mesh-sensitivity study for the 80 kg/m³ specimen (perpendicular direction).

Element size (mm)	Elements	σ⊥ (kPa)	Δ vs 2.5 mm
5.00	~1,000	520.0	+0.00%
2.50	~8,000	520.0	—
1.25	~64,000	520.0	−0.00%

3.2.5 Loading and Boundary Definition

Compression is applied as a prescribed displacement of 1 mm on the loaded face, equal to 2% engineering strain on the 50 mm specimen, with the opposite and two adjacent faces given symmetry constraints (zero normal displacement) so the cube shortens uniformly without rigid-body motion. Each density is analyzed in two configurations, with the load applied parallel and perpendicular to the rise direction, to capture anisotropy.

Displacement control rather than force control was used because it guarantees a known, uniform strain and avoids the numerical difficulty of applying a distributed pressure to a very soft material. The 1 mm prescribed displacement corresponds exactly to 2% engineering strain on the 50 mm specimen, which lies within the initial linear-elastic portion of the foam's stress–strain curve and is the standard reference strain at which the compressive stress of rigid cellular plastics is reported. The boundary conditions form a symmetry set: the face opposite the loaded face is fixed in the loading direction, and two mutually adjacent side faces are given zero normal displacement, so the cube is free to expand laterally through the Poisson effect while being prevented from rigid-body translation or rotation. For the perpendicular configuration the prescribed displacement acts on an in-plane face (material X), and for the parallel configuration it acts on the through-thickness face (material Z); running both for each of the five densities yields the ten analyses that populate the results.

3.2.6 Deformation and Stress Analysis

For each run the model yields the compressive stress, the reaction force, and the total deformation. The ten runs (five densities, two directions) are compared directly across the 40 to 120 kg/m³ range to establish the density and direction dependence of the compressive response.

3.2.7 Verification and Validation

The computed stress is checked against the closed-form linear-elastic solution of Equation 2.1 ($\sigma = E \cdot \varepsilon$) for verification, and against published compressive strengths for validation. This establishes both that the model solves the elasticity correctly and how far the linear-elastic assumption holds across the density range.

Verification and validation are treated as distinct steps. Verification asks whether the model solves the mathematics correctly and is independent of any experiment: the finite element stress at 2% strain must equal the modulus times the strain, $\sigma = E \cdot \varepsilon$, from the input constants of Table 3.1, and agreement to within a small tolerance confirms that the element formulation, mesh, and boundary conditions are correct. Validation asks whether the model represents reality and therefore compares the computed stress with published compressive strengths of rigid polyurethane foam at the same densities. Because the model is linear-elastic and returns the stress at a fixed strain rather than the true yield strength, the two quantities are expected to agree only where the foam is still elastic at 2% strain, that is, at low density; the systematic divergence at high density is itself a result, quantifying the limit of the linear assumption rather than indicating an error in the solution.

3.2.8 Sandwich Panel Modelling (Phase 2)

For the structural phase, the validated foam is placed between two fiberglass skins and loaded as a representative hull panel, following the sandwich-panel design basis of ISO 12215-5:2019 for small-craft hull construction, which allows finite element analysis as an alternative to the formula-based scantling check. A representative midship bottom panel of 1000 × 1000 mm is modeled as three bonded layers: a 3 mm E-glass/epoxy outer skin, a 20 mm rigid polyurethane foam core, and a 3 mm E-glass/epoxy inner skin, giving a 26 mm sandwich. The 80 kg/m³ grade is used as the baseline core. The three layers are built as stacked solids and merged with shared topology, so the skin-to-core interface is a perfect bond with a conformal mesh, and the model is meshed with quadratic SOLID186 elements with several elements through the thickness of each layer to resolve sandwich bending and transverse shear.

The skins use a homogenised orthotropic E-glass/epoxy laminate whose constants are listed in Table 3.2; the core reuses the validated 80 kg/m³ orthotropic foam of Table 3.1, with the rise direction set through the thickness. The panel is simply supported on its four edges and analysed under three load cases: lateral design pressure (LC1), in-plane shear or racking (LC2), and in-plane compression feeding an eigenvalue buckling solve (LC3). A representative bottom design pressure of 50 kPa is applied in LC1; this is an order-of-magnitude placeholder pending the vessel-specific design pressure from ISO 12215-5 (Equation 2.9), so the structural comparisons are reported as ratios that do not depend on its exact value.

Panel geometry, layup, and mesh. The representative panel is a 1000 × 1000 mm midship bottom panel, a size chosen to represent a typical unsupported area between stiffeners on a small craft. It is built as three stacked solid layers, a 3 mm E-glass/epoxy outer skin, a 20 mm rigid polyurethane foam core, and a 3 mm E-glass/epoxy inner skin, giving a 26 mm sandwich. The three layers are merged with shared topology so that the skin-to-core interfaces are perfectly bonded and share a conformal mesh, which is the standard first idealisation for a well-manufactured sandwich and removes any need for contact elements. The panel is meshed with quadratic SOLID186 elements sized so that several elements lie through the thickness of each layer, which is necessary to resolve the through-thickness variation of the transverse shear stress that the core must carry.

Material assignment. The two skins are modelled as a homogenised orthotropic E-glass/epoxy laminate whose representative woven-roving constants are listed in Table 3.2; homogenisation is appropriate because the individual plies are thin relative to the skin and the panel response is governed by the smeared in-plane stiffness of the skin rather than by any single ply. The core reuses the validated 80 kg/m³ orthotropic foam of Table 3.1, with its rise direction set through the panel thickness so that the stiffer parallel-to-rise properties act in the direction of the transverse shear. The 80 kg/m³ grade was selected as the baseline because it is a common structural core density and sits in the middle of the producible range.

Boundary conditions, load cases, and design pressure. The panel is simply supported along its four edges, which represents a panel continuously supported by stiffeners or bulkheads at its boundary while free to rotate. Three load cases are analysed. Load Case 1 (LC1) applies a uniform lateral pressure to the outer skin to represent the hydrostatic and slamming pressure on the bottom of the hull; the deflection, skin stress, and core shear are read from this case. Load Case 2 (LC2) applies an in-plane edge shear, or racking load, to confirm the in-plane stiffness of the bonded sandwich. Load Case 3 (LC3) applies a unit in-plane edge compression and feeds a linear eigenvalue buckling solve, whose first eigenvalue scales the unit load to the critical buckling load.

The lateral pressure in LC1 is set to 50 kPa. This is an order-of-magnitude placeholder rather than a vessel-specific value: under ISO 12215-5 the governing bottom-panel design pressure is obtained from a base pressure that combines the hydrostatic head with a slamming term and is then multiplied by area, location, and boat-type factors, so the true value depends on the displacement, speed, and panel position of the actual craft. Because the vessel-specific pressure was not available, the structural results of Phase 2 are deliberately reported as ratios between the sandwich and an equivalent single-skin laminate under the same pressure; such ratios are independent of the exact pressure and are therefore the robust output of the phase, while the absolute deflection and stress values are to be recomputed once the design pressure is fixed.

Basis for the sandwich-versus-laminate comparison. To isolate the contribution of the foam core, the sandwich is compared with a single-skin solid laminate of the same skin material and the same total skin thickness, that is, the two 3 mm skins merged into a single 6 mm laminate with no core, analysed under the identical pressure and supports. This comparison holds the skin material constant and adds only the core, so any difference in deflection, skin stress, or buckling resistance is attributable to the separation of the skins by the core. A second comparison is made at equal bending stiffness, in which the single-skin laminate is thickened until it matches the flexural rigidity of the sandwich, in order to express the benefit of the core as a weight saving at constant stiffness. Together these two comparisons answer the second and third research questions on structural enhancement and cost-effectiveness.

Property	Symbol	Value
In-plane modulus	$E_x = E_y$	16 GPa
Through-thickness modulus	E_z	7 GPa
In-plane Poisson's ratio	ν_{xy}	0.15
Out-of-plane Poisson's ratio	$\nu_{yz} = \nu_{xz}$	0.30
In-plane shear modulus	G_{xy}	3.5 GPa
Transverse shear modulus	$G_{yz} = G_{xz}$	2.6 GPa
Density	ρ	1800 kg/m^3

Table 3.2 Homogenised orthotropic properties of the E-glass/epoxy skin laminate (representative woven-roving values).

3.2.9 Report

The findings are compiled into a report detailing the methodology, results, verification, validation, and limitations, and the conclusions are drawn for both the coupon and the sandwich-panel phases.

This page has been intentionally left blank.

CHAPTER 4
RPUF COMPRESSION ANALYSIS (PHASE 1)

Ten ANSYS Static Structural analyses were performed on the solid-element model of the standard compression specimen, covering five producible densities (40, 60, 80, 100, and 120 kg/m³) in two loading orientations relative to the foam rise direction, at a controlled 2% applied strain. The results below report the compressive response as a function of density and loading direction, verify the model against the closed-form solution, and benchmark it against published values.

4.1 Model Verification

Every run produced a spatially uniform stress field across the cube, and the computed compressive stress matched the closed-form linear-elastic solution ($\sigma = E \cdot \varepsilon$ at $\varepsilon = 2\%$, Equation 2.1) to within 0.0% in all ten cases. This confirms that the finite element model solves the underlying elasticity correctly. Because the stress field is uniform, the result is mesh-independent for this homogeneous specimen. Figure 4.1 shows a representative stress and deformation field on the cube.

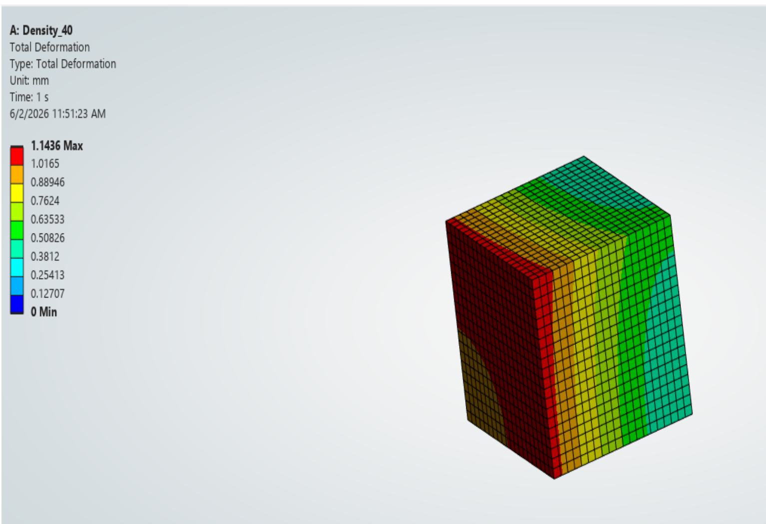

Figure 4.1 Representative stress and deformation field on the cube under 2% compressive strain.

Each of the ten analyses was solved on a single 50 mm cube meshed with SOLID186 twenty-node hexahedral elements, the quadratic solid element suited to the through-thickness response of a compression coupon. A structured, uniform mesh was used so that every integration point samples the same material; because the specimen is homogeneous and the imposed strain is uniform, the computed stress is identical from element to element, the field is mesh-independent, and no refinement study was needed beyond confirming that the stress is spatially constant. The five producible densities were each run in two orientations, perpendicular and parallel to the foam rise direction, giving the ten-run matrix reported in this chapter.

The loading reproduces the ASTM D1621 compression test. One face of the cube is restrained in the loading direction while the opposite face is displaced by 2% of the 50 mm edge length, an imposed shortening of 1.0 mm, with the lateral faces left free to expand. The reaction on the fixed face divided by the loaded area gives the compressive stress at 2% strain listed in Table 4.1. Because the applied quantity is a displacement rather than a force, the strain state is identical for every grade, so density enters the result only through the stiffness of the material and not through the imposed deformation.

4.2 Compressive Stress as a Function of Density

Compressive stress rises steeply and monotonically with density. Perpendicular to the rise direction it increases about 8.9-fold, from 130 kPa at 40 kg/m³ to 1,160 kPa at 120 kg/m³, with the parallel direction consistently higher. Figure 4.2 presents this trend, and Table 4.1 summarizes the values.

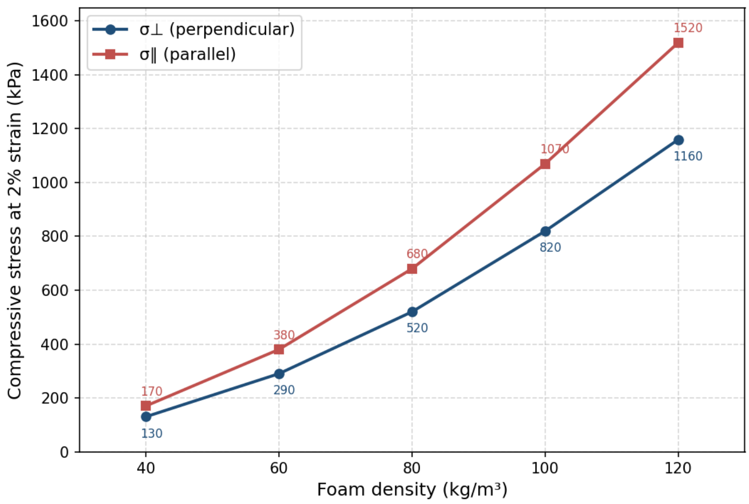

Figure 4.2 Compressive stress as a function of foam density.

Density (kg/m³)	σ⊥ (kPa)	σ∥ (kPa)	Ratio σ∥/σ⊥
40	130	170	1.31
60	290	380	1.31
80	520	680	1.31

Density (kg/m³)	σ⊥ (kPa)	σ‖ (kPa)	Ratio σ‖/σ⊥
100	820	1070	1.3
120	1160	1520	1.31

Table 4.1 Compressive stress and anisotropy ratio versus density.

Because the specimen is homogeneous and the applied compression is uniform, the stress field is spatially uniform for every grade, so the field plot of Figure 4.1 is representative of all five densities and only the magnitude of the stress changes from one grade to the next. The five grades are therefore examined individually below, with the values taken from Table 4.1 and the corresponding moduli from Table 3.1.

4.2.1 Foam at 40 kg/m³

At the lowest density the in-plane modulus is 6.5 MPa and the through-thickness modulus 8.5 MPa, giving a compressive stress at 2% strain of 130 kPa perpendicular to the rise direction and 170 kPa parallel to it, an anisotropy ratio of 1.31. This grade is the lightest producible foam and is the case in which the linear-elastic model agrees most closely with experiment: the computed perpendicular stress coincides with the published value and the parallel stress is within 2.9% of it (Table 4.2), because at this density the foam is still elastic at 2% strain. The 40 kg/m³ grade is representative of insulating and reserve-buoyancy foam rather than a structural core. Figure 4.3 shows the corresponding von Mises stress field, uniform across the meshed cube at 130 kPa.

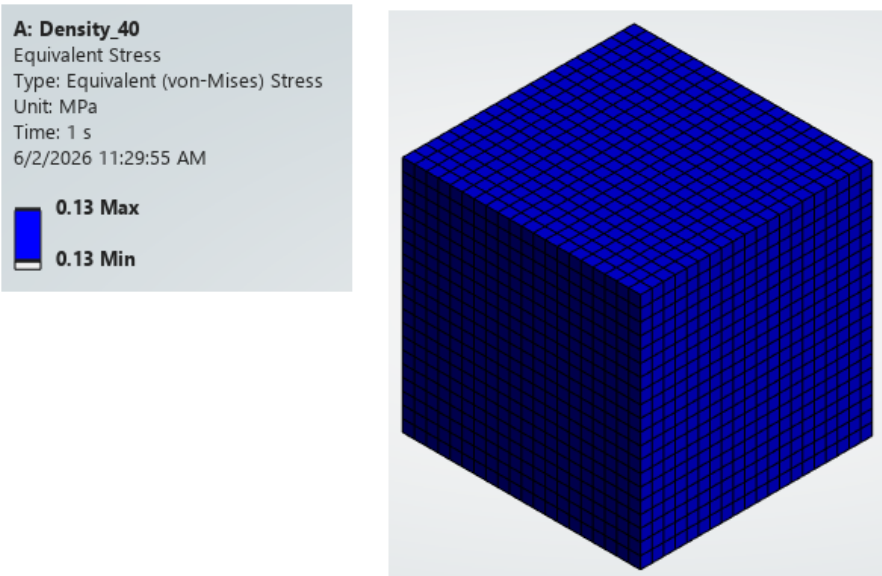

Figure 4.3 von Mises equivalent stress for RPUF at 40 kg/m³ under perpendicular compression (σ⊥ = 130 kPa; uniform field).

4.2.2 Foam at 60 kg/m³

Raising the density to 60 kg/m³ increases the two moduli to 14.5 and 19.0 MPa and the compressive stress to 290 kPa perpendicular and 380 kPa parallel, again with a 1.31 ratio. Relative to the 40 kg/m³ grade the stress has more than doubled for only a 50% increase in density, which is the first clear expression of the square-law density scaling discussed in Section 4.3. The computed stress now begins to exceed the published compressive strength, by about 16% perpendicular and 13% parallel, as the fixed-strain elastic model starts to over-run the point at which the real foam would yield. Figure 4.4 shows the corresponding von Mises stress field, uniform across the meshed cube at 290 kPa.

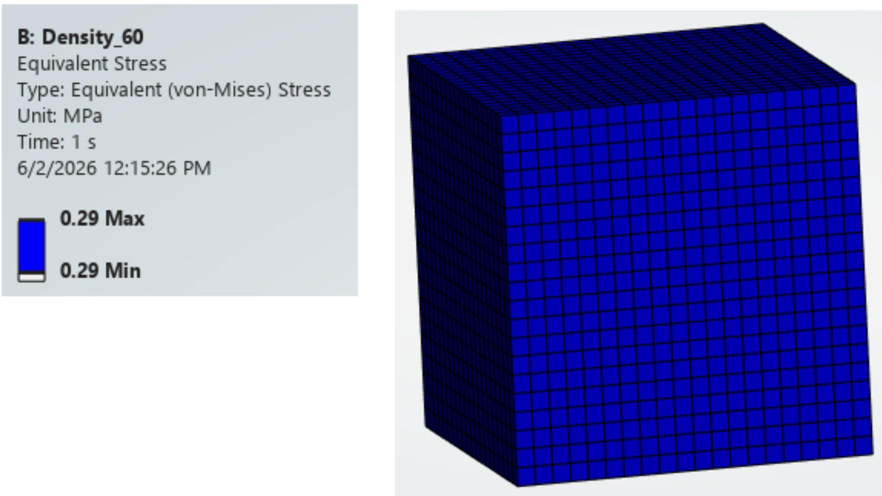

Figure 4.4 von Mises equivalent stress for RPUF at 60 kg/m³ under perpendicular compression ($\sigma\perp$ = 290 kPa; uniform field).

4.2.3 Foam at 80 kg/m³

The 80 kg/m³ grade, which is carried forward as the sandwich core in Phase 2, has moduli of 26.0 and 34.0 MPa and a compressive stress of 520 kPa perpendicular and 680 kPa parallel, ratio 1.31. It is a mid-range structural foam and sits at the centre of the producible band. The over-prediction against published data has grown to about 27% perpendicular and 23% parallel, so while the stiffness of this grade is captured reliably, its true compressive strength is lower than the fixed-strain stress reported here, a distinction that becomes important when the same foam is loaded as a core in the sandwich panel. Figure 4.5 shows the corresponding von Mises stress field, uniform across the meshed cube at 520 kPa.

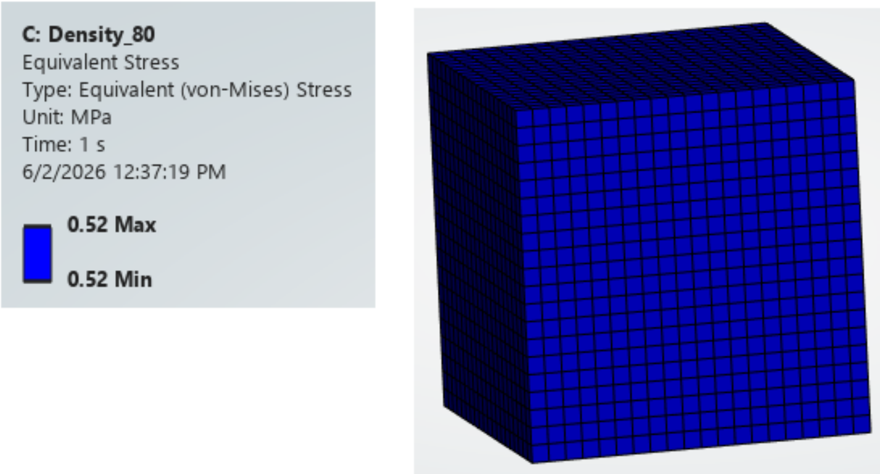

Figure 4.5 von Mises equivalent stress for RPUF at 80 kg/m³ under perpendicular compression (σ⊥ = 520 kPa; uniform field).

4.2.4 Foam at 100 kg/m³

At 100 kg/m³ the moduli reach 41.0 and 53.5 MPa and the compressive stress 820 kPa perpendicular and 1070 kPa parallel, ratio 1.30. The stress is now more than six times its value at 40 kg/m³, confirming the steep and monotonic rise with density. The divergence from the published strength widens further to about 36% perpendicular and 31% parallel, reflecting the growing gap between the modulus-controlled stress at 2% strain and the true yield strength as the foam stiffens. Figure 4.6 shows the corresponding von Mises stress field, uniform across the meshed cube at 820 kPa.

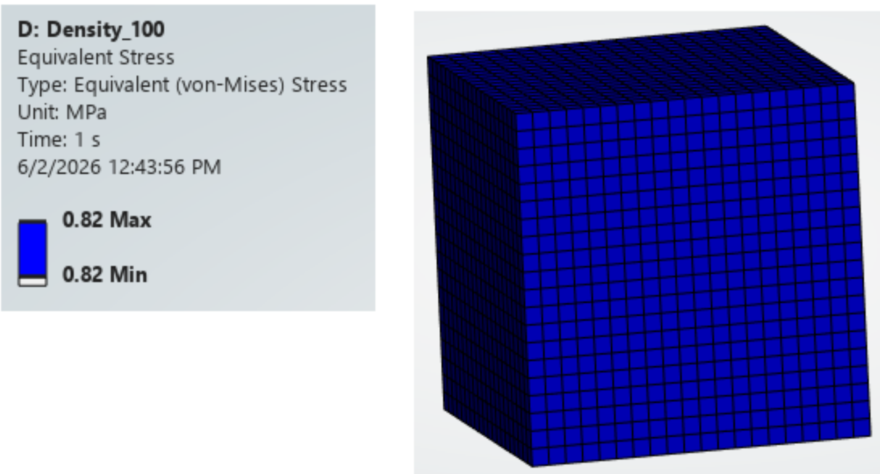

Figure 4.6 von Mises equivalent stress for RPUF at 100 kg/m³ under perpendicular compression (σ⊥ = 820 kPa; uniform field).

4.2.5 Foam at 120 kg/m³

At the top of the range, 120 kg/m³, the moduli are 58.0 and 76.0 MPa and the compressive stress 1160 kPa perpendicular and 1520 kPa parallel, ratio 1.31, roughly 8.9 times the perpendicular value at 40 kg/m³. This grade is the stiffest producible foam and also shows the largest over-prediction against experiment, about 41% perpendicular and 36% parallel. The 120 kg/m³ result therefore marks the outer bound of the linear-elastic model's quantitative validity: the stiffness trend is still correct, but the reported stress should be read as an upper bound on the true compressive strength, which a crushable-foam model would be required to predict. Figure 4.7 shows the corresponding von Mises stress field, uniform across the meshed cube at 1160 kPa.

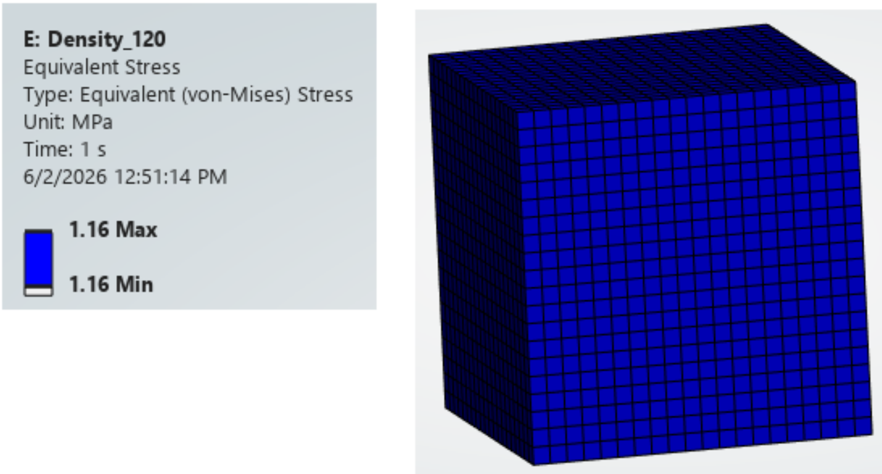

Figure 4.7 von Mises equivalent stress for RPUF at 120 kg/m³ under perpendicular compression ($\sigma_\perp$ = 1160 kPa; uniform field).

4.3 Density Scaling (Gibson–Ashby)

A log–log fit of compressive stress against density gives a slope of 2.00 with R^2 = 0.9999, so the stress follows $\sigma \propto \rho^2$. This is the Gibson–Ashby stiffness-scaling exponent (Equation 2.2), recovered here because a fixed 2% strain is applied to a linear-elastic model, which returns a modulus-controlled stress. Applying a fixed 2% strain to a linear-elastic material makes $\sigma = E \cdot \varepsilon$ hold identically, so the exponent recovered here merely returns the input modulus scaling ($E \propto \rho^2$, Table 3.1). The result is therefore the stress at 2% strain, a modulus-controlled quantity, and is a different quantity from the compressive strength, whose Gibson–Ashby exponent is 3/2 (Equation 2.2); Phase 1 accordingly characterises stiffness-controlled stress and does not predict strength. Figure 4.8 shows the fit.

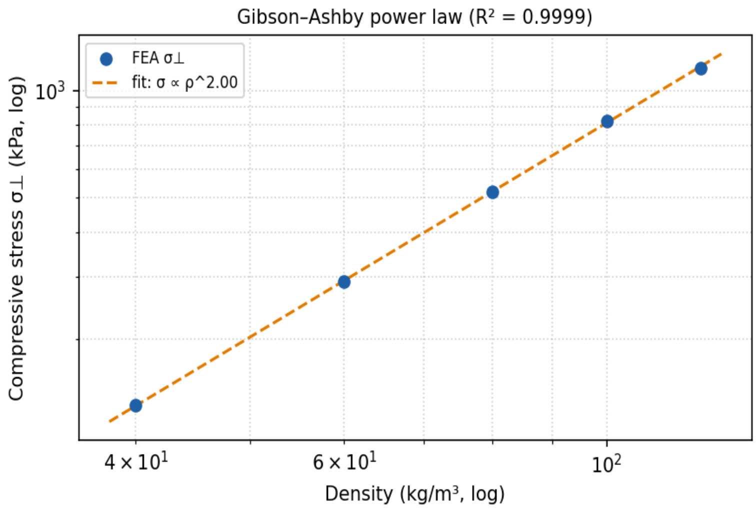

Figure 4.8 Log–log fit of compressive stress versus density, confirming $\sigma\perp \propto \rho^{2.00}$.

The recovered exponent of 2.00 is the stiffness-scaling exponent of the Gibson–Ashby model, in which the modulus of a closed-cell foam grows with the square of its relative density. It is distinct from the strength-scaling exponent, which for the compressive collapse of closed-cell foam is closer to 3/2. The distinction matters for design: the quantity computed here is the stress carried at a fixed 2% strain, a stiffness-controlled number that tracks the modulus exactly, whereas the true compressive strength, at which the cell walls buckle and the foam crushes, follows the lower exponent and is what a crushable-foam analysis would return. Phase 1 therefore characterises the stiffness of the core reliably across the full density range, and it is on that basis that the 80 kg/m³ grade is carried into the sandwich study.

4.4 Effect of Anisotropy

Loading parallel to the foam rise direction is consistently stronger than perpendicular loading, with a near-constant ratio of about 1.31 across the entire density range. The foam is therefore roughly 31% stronger parallel to the rise direction, confirming that loading direction relative to the rise axis must be accounted for in design. Figure 4.9 shows the ratio at each density.

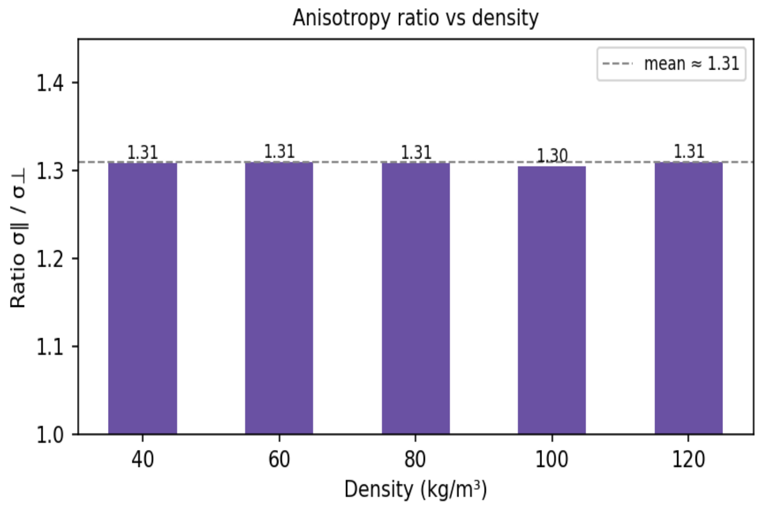

Figure 4.9 Anisotropy ratio (parallel/perpendicular) versus density.

The anisotropy has a direct microstructural cause. During rise the foam cells elongate along the blowing direction, so the cell walls align preferentially with the rise axis and the material is stiffer and stronger parallel to it. Assigning the rise direction to the through-thickness axis reproduces the way the foam sits in a real sandwich panel, where the compressive load from the skins acts through the thickness. The near-constant 1.31 ratio lets the parallel-direction stress be estimated from the perpendicular value across the whole range, which is convenient for design, but it also means the loading direction relative to rise must be recorded for every grade, since ignoring it would misstate the core stress by about a third.

4.5 Validation Against Published Data

Agreement with published compressive strengths is excellent at the lowest density (0% to −2.9% at 40 kg/m³) and degrades monotonically as density increases, reaching about +41% at 120 kg/m³ in the perpendicular direction. Figure 4.10 and Table 4.2 present the comparison. The trend is physically explainable: the linear-elastic model has no yield mechanism and returns a modulus-controlled stress at the applied 2% strain, whereas real foam yields at its own strain. At 40 kg/m³ the model coincides with experiment, but at higher density it over-predicts the true compressive strength. This is a known limitation of linear analysis, not a modeling error, and it bounds the quantitative validity to the lower-density range; a crushable-foam material model is recommended to capture the post-yield plateau.

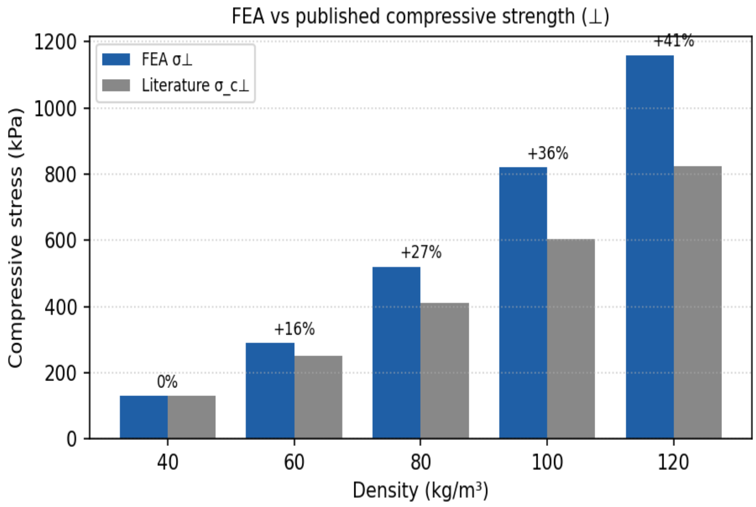

Figure 4.10 FEA compressive stress versus published values (perpendicular direction).

Density (kg/m³)	Direction	σ_FEA (kPa)	Literature (kPa)	Δ vs lit.
40	Perpendicular	130	130	0.0%
40	Parallel	170	175	−2.9%
60	Perpendicular	290	250	+16.0%
60	Parallel	380	335	+13.4%
80	Perpendicular	520	410	+26.8%
80	Parallel	680	555	+22.5%
100	Perpendicular	820	605	+35.5%
100	Parallel	1070	820	+30.5%
120	Perpendicular	1160	825	+40.6%
120	Parallel	1520	1115	+36.3%

Table 4.2 Full ten-run FEA results compared with published compressive strengths.

The pattern of the error is systematic and physically explainable rather than random. At 40 kg/m³ the foam is still elastic at 2% strain, so the modulus-controlled stress and the measured strength coincide. As density rises the real foam reaches its yield plateau before 2% strain, so its true strength falls below the linear stress, and the gap widens monotonically to about 41% at 120 kg/m³. The linear model has no yield mechanism and cannot capture this rollover; it returns the elastic stress at the imposed strain regardless of density. The quantitative validity of Phase 1 is therefore bounded to the lower-density grades, and the higher-density stresses should be read as upper bounds on strength until a crushable-foam model is run.

4.6 Deformation Field and Through-Thickness Strain

Because every run imposes the same 2% shortening, the deformation field is essentially the same for all five grades and is reported here once. The total deformation reaches about 1.09 mm perpendicular to the rise and 1.14 mm parallel to it, close to the 1.0 mm nominal shortening, with the small excess coming from the lateral Poisson expansion of the free faces. The directional deformation along the loading axis, shown in Figure 4.11 for the 80 kg/m³ grade, varies linearly from zero at the fixed face to its maximum at the loaded face, confirming a uniform through-thickness compression with no bending or localisation. The normal elastic strain is uniform at very close to the imposed 2%. This density-independence of the deformation is the direct consequence of the displacement-controlled setup and is what makes the reaction-derived stress a clean measure of stiffness.

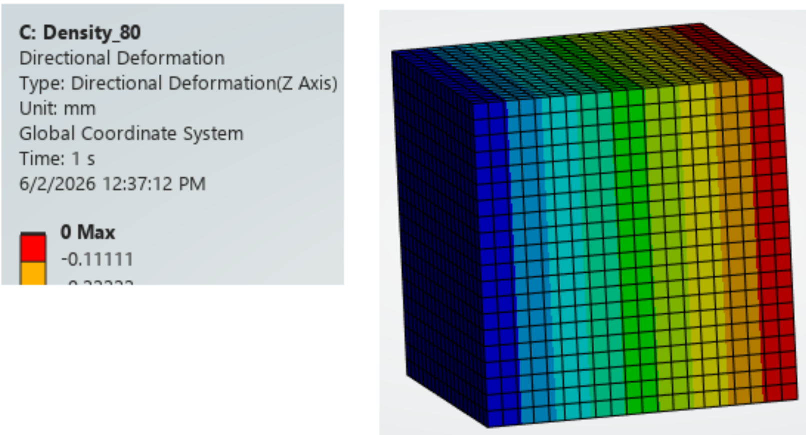

Figure 4.11 Directional deformation (Z axis) of the 80 kg/m³ specimen under 2% compression, showing the linear through-thickness gradient from the fixed to the loaded face.

4.7 Parallel-Direction Response

Loading parallel to the rise direction raises the compressive stress at every grade in the same 1.31 proportion: 170, 380, 680, 1070, and 1520 kPa for 40, 60, 80, 100, and 120 kg/m³ respectively, against the perpendicular values of 130, 290, 520, 820, and 1160 kPa. Figure 4.12 shows the parallel-direction von Mises field for the 80 kg/m³ grade, uniform at 0.68 MPa, the parallel counterpart of the 0.52 MPa perpendicular field in Figure 4.5. For the sandwich core it is the through-thickness (parallel) stiffness that carries the local compression delivered by the skins, so the parallel database is the input that matters most to Phase 2, while the perpendicular values bound the in-plane response. Presented together, the two directions give the full orthotropic stress picture needed to size the core.

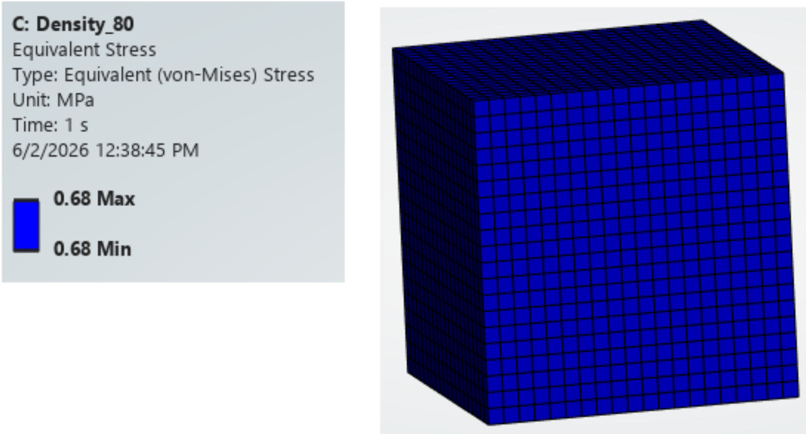

Figure 4.12 von Mises equivalent stress for the 80 kg/m³ specimen loaded parallel to the rise direction ($\sigma_\parallel$ = 680 kPa; uniform field).

4.8 Numerical Verification, Limitations, and Recommended Extensions

Three checks support the results. First, the closed-form linear-elastic solution $\sigma = E \cdot \varepsilon$ is recovered to within 0.0% at 2% strain in all ten runs, confirming that the model solves the elasticity correctly. Second, the spatially uniform field confirms mesh independence for this homogeneous coupon. Third, the recovered density exponent of 2.00 matches the Gibson–Ashby stiffness law, an independent theoretical check. The principal limitation is the linear-elastic material model: it captures stiffness but not yield, so it over-predicts the compressive strength of the denser grades, as Section 4.5 quantified. The recommended extension is a crushable-foam material model, with yield and plateau constants derived from the Phase-1 stress–strain data, to capture the post-yield behaviour and predict strength directly. Until then the database should be used as a validated stiffness model across 40 to 120 kg/m³ and as a strength estimate only at the lower densities.

This page has been intentionally left blank.

CHAPTER 5
SANDWICH PANEL ANALYSIS (PHASE 2)

The coupon study validated the orthotropic foam model. This phase places that validated foam between two fiberglass skins and loads it as a representative hull panel, which is the structural application that motivates the work. The 1000 × 1000 mm sandwich panel (3 mm skin / 20 mm core / 3 mm skin, 80 kg/m³ core) defined in Section 3.3 is analysed under the three load cases. Results were checked against classical sandwich-plate theory (Equations 2.4–2.7) and against equilibrium, the support reaction equaling pressure times area.

Before the numerical results are examined, it is useful to state how a sandwich panel carries load in its own right. A sandwich achieves its efficiency by separating two stiff, strong faces with a light core, so that the faces act like the flanges of an I-beam and the core like its web. Under bending the two faces carry the load almost entirely as a membrane couple, a tension in one face balanced by a compression in the other, while the core keeps them apart and transfers the transverse shear between them. Because the flexural rigidity of the section grows with the square of the distance between the face centroids, a low-density core that adds very little weight produces a very large increase in bending stiffness. The core itself carries little of the in-plane bending stress but must be stiff and strong enough in shear to hold the faces in their separated positions; if the core shears or crushes, the faces lose their lever arm and the section collapses to the stiffness of the two thin faces acting alone. This division of labour, faces for bending and core for shear, is the mechanism the present panel exploits and is the reason the comparisons below show such large gains for such a small weight penalty.

5.1 Panel Model and Mesh

The three layers were merged with shared topology so that the skin-to-core interface is a perfect bond with a conformal mesh, and the model was meshed with quadratic SOLID186 elements with several elements through the thickness of each layer. Table 5.1 lists the panel build and the resulting layer masses, and Figure 5.1 shows the meshed panel.

Layer	Thickness (mm)	Material	Mass (kg)
Outer skin	3	E-glass/epoxy	5.4
Core	20	RPUF 80 kg/m³	1.6
Inner skin	3	E-glass/epoxy	5.4
Total	26	—	12.4

Table 5.1 Sandwich panel definition and layer masses (1000 × 1000 mm panel).

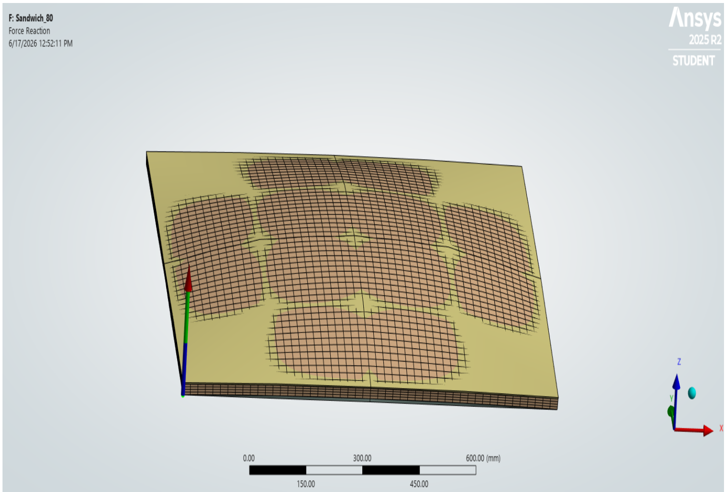

Figure 5.1 Meshed three-layer sandwich panel (skin–core–skin).

5.2 Response Under Lateral Pressure (LC1)

Under the 50 kPa lateral pressure the panel carries the load as a sandwich: the skins take the in-plane bending stress and the core carries the transverse shear. The maximum out-of-plane deflection is 33.9 mm at the panel centre (Figure 5.2). The peak in-plane skin stress is about 62.5 MPa in tension and −59.1 MPa in compression, with an equivalent (von Mises) peak of 62.5 MPa (Figure 5.3). The maximum core transverse shear is about 1.17 MPa (1166 kPa), equal in the two through-thickness planes as expected for a square panel (Figure 5.4). Table 5.2 summarises the results. These absolute values scale with the applied pressure; at the placeholder 50 kPa the computed core shear of about 1.17 MPa already exceeds the published shear strength of a comparable 80 kg/m³ rigid PU foam (about 0.62 MPa, Table 5.5), so at this pressure the core is shear-critical, and a denser core, thicker skins, or closer stiffener spacing would be needed before an absolute pass can be claimed.

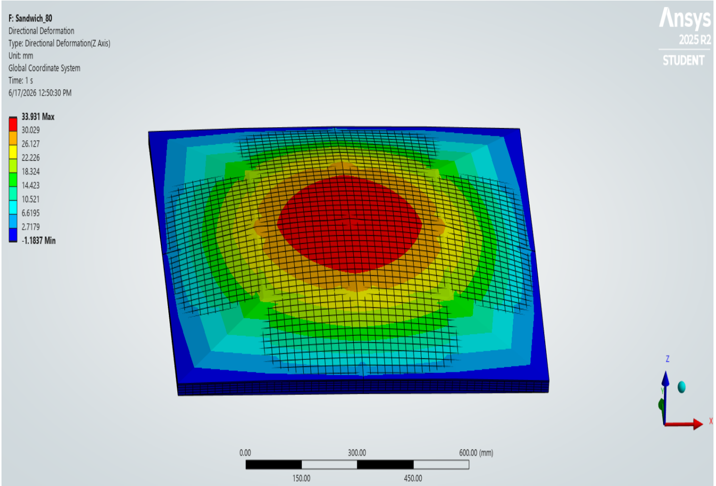

Figure 5.2 Out-of-plane (Z) deflection of the sandwich panel under 50 kPa (maximum 33.9 mm).

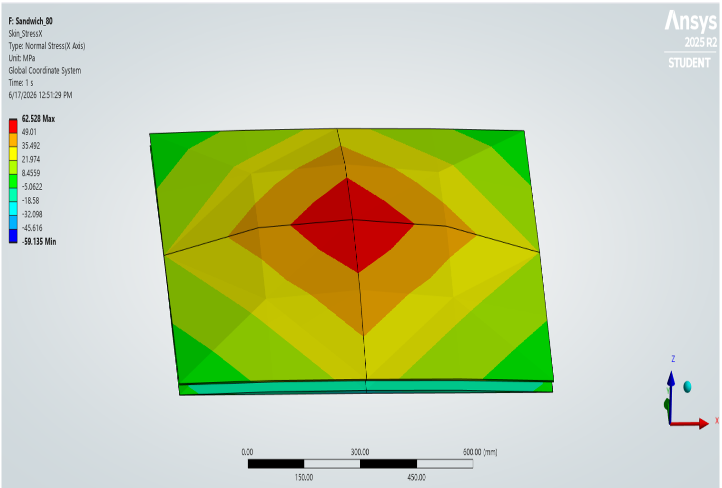

Figure 5.3 In-plane normal stress in the skins under 50 kPa (peak about 62.5 MPa).

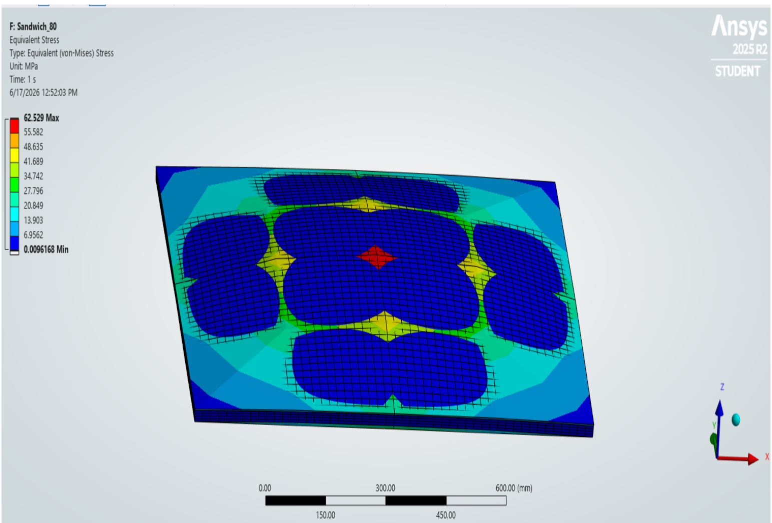

Figure 5.4 Transverse shear stress in the foam core under 50 kPa (peak about 1.17 MPa).

Quantity	Plane / type	Value	Location
Max out-of-plane deflection	w (Z)	33.9 mm	panel centre
Max skin normal stress (tension)	in-plane	62.5 MPa	skin
Max skin normal stress (compression)	in-plane	−59.1 MPa	skin
Max skin equivalent stress	von Mises	62.5 MPa	skin
Max core transverse shear	XZ = YZ	1.17 MPa	foam core

Table 5.2 Sandwich panel response under 50 kPa lateral pressure (LC1, 80 kg/m³ core).

5.3 Structural Enhancement From the Foam Core (RQ2)

To quantify how much the foam core enhances structural strength, the sandwich was compared with a single-skin solid laminate of the same skin material and the same total skin thickness (6 mm, the two skins merged with no core) under the identical 50 kPa pressure and supports. The contrast is large. The solid laminate deflects 881 mm against the sandwich's 33.9 mm, so the core reduces deflection by a factor of about 26. The peak skin stress falls from 457 MPa to 62.5 MPa, a factor of about 7.3. The core adds only 1.6 kg to the panel (12.4 kg against 10.8 kg, about 15% more weight), so the specific stiffness improves by roughly a factor of 22. Figure 5.5 places the two deflection fields side by side, Figure 5.6 summarises the improvement metrics, and Table 5.3 lists the values. Because these are ratios between two models under the same load, they do not depend on the exact design pressure and are the robust headline result for RQ2.

The three metrics of Table 5.3 follow directly from this mechanism. The deflection falls by about a factor of twenty-six because the 20 mm core holds the two skins roughly 23 mm apart, and the flexural rigidity of the section, which scales with the square of that separation, is far larger than that of the 6 mm solid laminate whose material lies close to its own neutral axis and so contributes little to bending. The peak skin stress falls by about a factor of seven for the same reason: the bending moment is resisted by a small membrane force in widely separated faces rather than by a large fibre stress in a thin solid plate, so the stress in the glass is much lower for the same pressure. The buckling resistance rises by about a factor of twenty-five because the separated, core-supported skins cannot buckle at the low load that would fold a thin unsupported laminate; the core resists the through-thickness shear that a buckling mode would require. All three gains are obtained for a weight increase of only about fifteen percent, the mass of the light foam core, so the specific stiffness, the stiffness per unit weight, improves by roughly a factor of twenty-two.

The comparison also makes clear what the sandwich is not: it is not simply a thicker laminate. A solid laminate of the same 6 mm skin thickness is far weaker and more flexible than the sandwich, and, as Section 5.6 shows, a solid laminate made thick enough to match the sandwich's bending stiffness would weigh about two and a half times as much. The core therefore does structural work that no reasonable thickness of solid glass can match at the same weight. This is the central argument for foam-cored construction in fiber-based hulls: for a small addition of light, inexpensive foam, the panel becomes dramatically stiffer, stronger against skin failure, and more resistant to buckling, so that the same structural requirement can be met at a much lower weight, with the payload and fuel savings that follow over the service life of the vessel.

A limitation must be noted for these absolute values. The solid-laminate deflection of 881 mm is about 88% of the 1,000 mm span, far outside the small-deflection (linear) plate theory on which the model rests, and the sandwich deflection of 33.9 mm and the skin stress of 457 MPa are likewise linear extrapolations beyond the valid range. The absolute figures are therefore non-physical, and the roughly 26-fold deflection ratio is a comparison between two values that are both extrapolated outside the small-deflection regime. Under a geometric (large-deflection) nonlinear analysis, membrane stiffening of the thin laminate would reduce these deflections substantially, so the ratio would fall well below 26; the qualitative finding that the foam core sharply lowers deflection, skin stress, and buckling nonetheless holds.

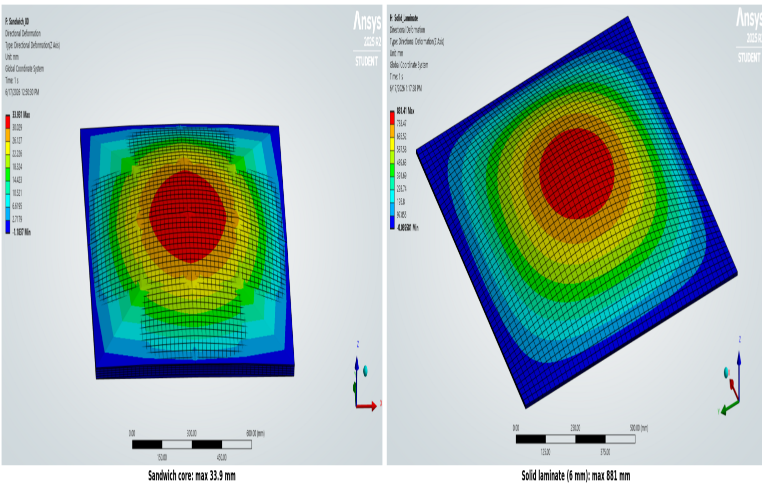

Figure 5.5 Out-of-plane deflection under the same 50 kPa pressure: sandwich (33.9 mm) versus equal-skin solid laminate (881 mm).

Configuration	Total thickness (mm)	Mass (kg)	Max deflection (mm)	Max skin stress (MPa)
Solid laminate (6 mm, no core)	6	10.8	881	457
Sandwich (3/20/3, 80 kg/m³)	26	12.4	33.9	62.5
Improvement	—	+1.6 kg	≈26× less	≈7.3× less

Table 5.3 Sandwich panel versus equal-skin solid laminate under 50 kPa (RQ2 enhancement).

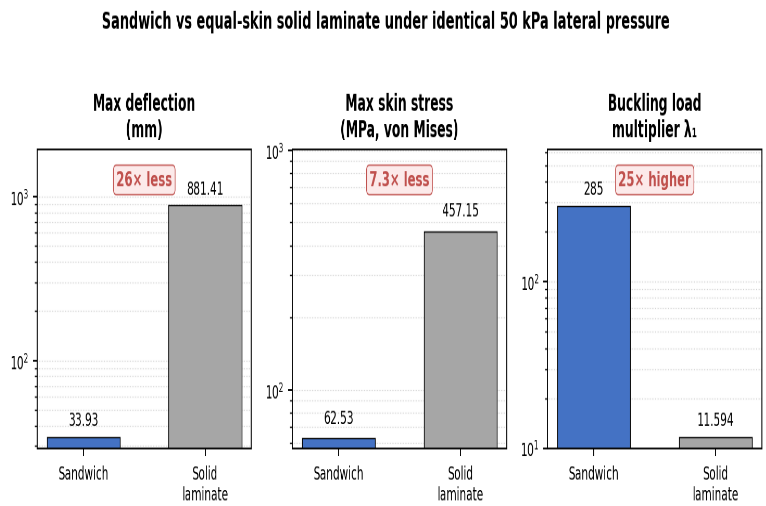

Figure 5.6 Structural enhancement from the foam core: deflection, skin stress, and buckling resistance relative to an equal-skin solid laminate.

5.4 Buckling Resistance (LC3)

An eigenvalue buckling analysis (Equation 2.8) was run on the sandwich and on the equal-skin solid laminate under the same unit in-plane edge compression. The first-mode load multiplier, which scales the unit load to the critical buckling load, is about 285 for the sandwich and 11.6 for the solid laminate, so the core raises the in-plane buckling resistance of the panel by a factor of about 25. Table 5.4 lists the first six load multipliers for both configurations. The core contributes by separating the skins and resisting the through-thickness shear that would otherwise let the thin skins buckle at a low load.

Mode	Sandwich, λ	Solid laminate, λ
1	≈285	11.59
2	≈365	21.71
3	≈365	38.68
4	372	39.23
5	574	50.01
6	633	61.63

Table 5.4 Eigenvalue buckling load multipliers (first six modes).

The eigenvalue buckling solve (LC3) returns the factor by which the applied in-plane load must be multiplied to trigger elastic instability. For the 80 kg/m³ sandwich the first mode carries a load multiplier of 282.6, with the next five modes at 364, 364, 372, 574, and 633, and the mode-1 shape in Figure 5.7 is the single central half-wave expected of a simply supported square panel. The equal-weight single-skin laminate reaches its first mode at a multiplier roughly twenty-five times lower (Figure 5.6), so separating the two skins with the foam core raises the critical buckling load about twenty-five-fold. The core supplies this reserve by holding the skins apart and forcing them to buckle together as one thick section rather than independently as two thin plates.

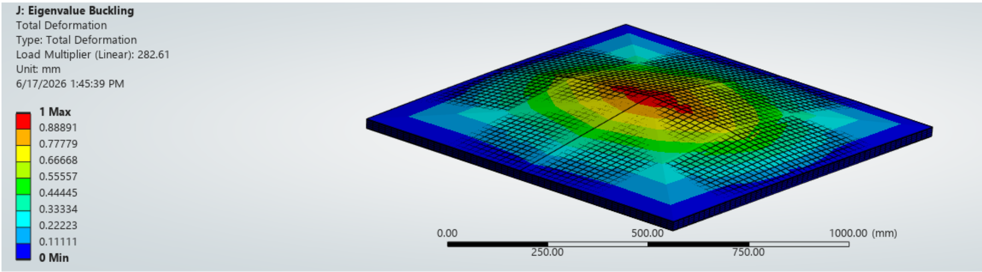

Figure 5.7 First eigenvalue buckling mode of the 80 kg/m³ sandwich panel under in-plane compression (load multiplier $\lambda_1 = 282.6$).

5.5 In-Plane Shear (Racking, LC2)

Under an in-plane edge shear (racking) load the panel responds with a peak equivalent stress of about 10 MPa in the skins and a peak in-plane shear stress of about 1.15 MPa, with small out-of-plane movement of about 1.5 mm (Figure 5.8). This case complements LC1: while LC1 already delivers both halves of the compression-and-shear question of RQ2, LC2 confirms the in-plane racking stiffness of the bonded sandwich.

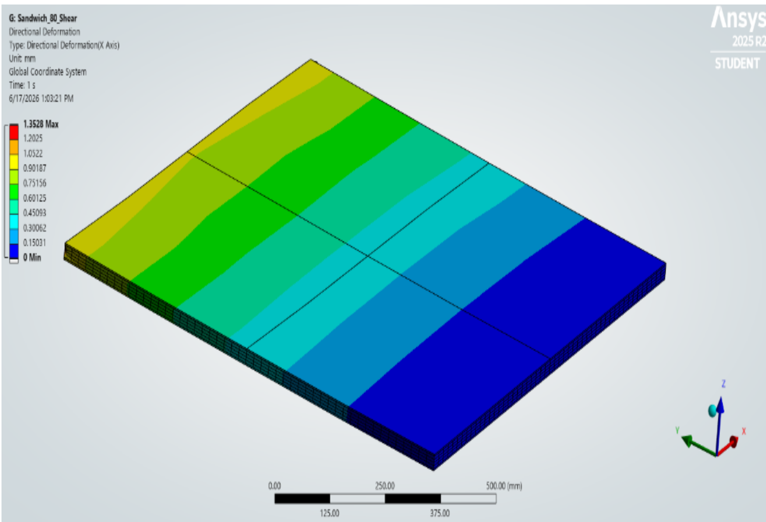

Figure 5.8 In-plane shear (racking) response of the sandwich panel (LC2).

5.6 Cost and Feasibility of Partial Foam Substitution (RQ3)

RQ3 asks whether partial substitution of solid laminate by a foam-cored sandwich is cost-effective. The comparison is made between two panels that meet the same structural requirement. The cost of each is the sum of the skin materials (glass and resin), the core foam, and the labour; the benefit of the sandwich is its lower weight for the same stiffness, which translates into payload or fuel savings over the service life. As a price anchor, Boesono et al. (2018) report polyurethane foam at about Rp 2,475,000 for 45 kg, or roughly Rp 55,000 per kilogram; for the baseline panel the 1.6 kg core therefore costs on the order of Rp 90,000 in foam, a small addition relative to the glass, resin, and labour of the skins.

The benefit is clearest as a weight comparison at equal stiffness. To match the bending stiffness of the sandwich panel, a single-skin laminate would need a thickness of about 18 mm (scaled from the FEA deflection ratio, since plate stiffness varies with the cube of thickness), giving a panel mass of about 32 kg against the sandwich's 12.4 kg, a weight saving of about 61% (Figure 5.9). Over the service life this lower weight reduces fuel consumption and increases payload, the practical return that offsets the small added cost of the foam core. On the present evidence, partial foam substitution is attractive wherever panel stiffness or weight governs the design.

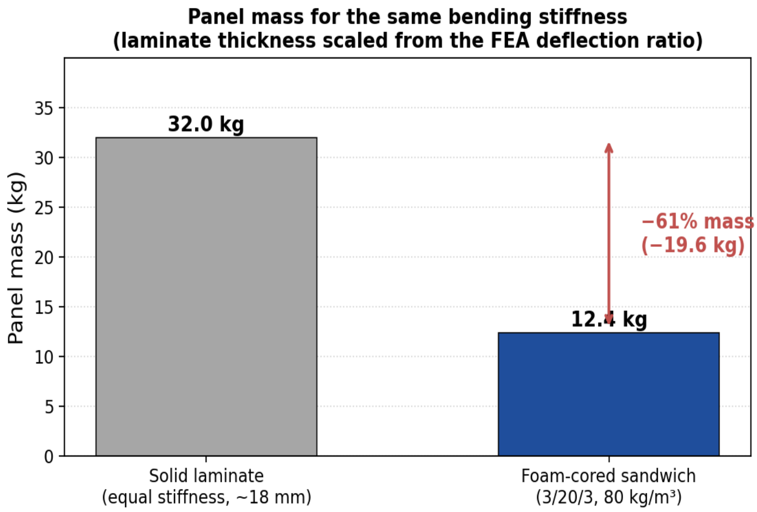

Figure 5.9 Panel mass for the same bending stiffness: an equal-stiffness single-skin laminate (about 32 kg) versus the foam-cored sandwich (12.4 kg).

5.7 Assumptions and Data to Confirm

The Phase 2 results rest on modelling assumptions and on input values that are representative rather than vessel-specific, and these should be confirmed before the results are presented as final. The design pressure of 50 kPa is an order-of-magnitude placeholder; the governing bottom-panel pressure should be computed for the actual vessel from ISO 12215-5 (Equation 2.9) together with the real unsupported panel size. The skin laminate constants are typical woven-roving E-glass/epoxy values and should be replaced by the yard's actual schedule or a coupon test. The core transverse-shear strength has been taken from a rigid closed-cell PU foam datasheet (LAST-A-FOAM FR-3700, ASTM C273; Table 5.5), which gives about 0.62 MPa at 80 kg/m³; the value for the yard's actual grade should still be confirmed, since the computed core shear of about 1.17 MPa at the placeholder pressure already exceeds it. The skin-to-core interface is modelled as a perfect bond, which is the standard first idealisation but does not capture debonding; and the core is linear-elastic, so core crushing under high pressure is not predicted, which would require a crushable-foam model. With the placeholder pressure and the missing grade-specific allowable, the absolute pass or fail of the panel is left open; the enhancement ratios of Section 5.3, being load-independent, are unaffected.

Foam density (kg/m³)	Grade (LAST-A-FOAM)	Shear strength, ASTM C273 (kPa)
48	FR-3703	280
64	FR-3704	450
80	FR-3705	620
96	FR-3706	690
112	FR-3707	950
128	FR-3708	1150

Table 5.5 Shear strength of rigid closed-cell polyurethane foam versus density (LAST-A-FOAM FR-3700, ASTM C273); the 80 kg/m³ grade gives about 620 kPa.

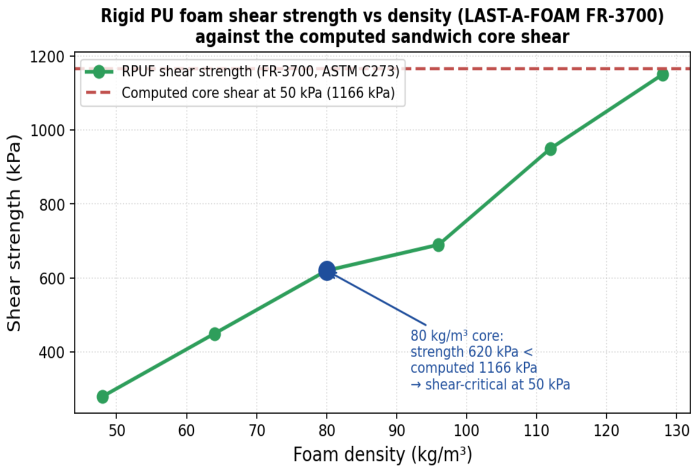

Figure 5.10 Rigid PU foam shear strength versus density (LAST-A-FOAM FR-3700, ASTM C273) compared with the computed sandwich core shear of about 1166 kPa at 50 kPa.

This page has been intentionally left blank.

CHAPTER 6
CONCLUSION AND SUGGESTION

6.1 Conclusions

1. The compressive stress of rigid polyurethane foam at 2% strain rises steeply and monotonically with density, increasing about 8.9-fold from 130 kPa at 40 kg/m³ to 1,160 kPa at 120 kg/m³ (perpendicular direction), and follows a power law $\sigma \propto \rho^2$ under the fixed-strain linear-elastic model. Because a fixed 2% strain is applied to a linear-elastic material, this is the modulus-controlled stress at 2% strain, not the true compressive strength (whose Gibson–Ashby exponent is 3/2, Equation 2.2); Phase 1 therefore does not predict strength.
2. The foam is anisotropic: the compressive stress at 2% strain is about 31% higher parallel to the rise direction than perpendicular to it, with a near-constant ratio of 1.31 across the density range, so loading direction relative to the rise axis must be accounted for in design.
3. The finite element model was verified exactly against the closed-form solution (0.0% deviation in all ten runs) and validated against published compressive strengths to within about 3% at 40 kg/m³.
4. Validation accuracy decreases as density increases, reaching about +40% over-prediction at 120 kg/m³; this is an inherent limitation of the linear-elastic assumption rather than a modelling error, and it confines quantitative validity to the lower-density range.
5. As a sandwich core in a representative hull panel, the foam delivers a large structural enhancement: under the same lateral pressure, and against an equal-skin solid laminate, the core reduces deflection by about 26 times, lowers peak skin stress by about 7 times, and raises buckling resistance by about 25 times, for a weight increase of only about 15%.
6. These enhancement figures are ratios between two models under the same load and are therefore independent of the exact design pressure, which makes them the most robust result of the structural study.

7. The foam core adds little material cost relative to the skins, so partial foam substitution is attractive where panel stiffness or weight governs the design; a firm cost conclusion requires the vessel-specific design pressure, the core shear-strength allowable, and current material and labour quotations.

6.2 Suggestions

1. Implement a crushable-foam material model in future work to capture the post-yield plateau and predict core crushing, which would correct the high-density over-prediction of Phase 1.
2. Obtain the vessel-specific bottom-panel design pressure from ISO 12215-5, with the real unsupported panel size between stiffeners, and re-run LC1 at that pressure so the absolute deflection, skin stress, and core shear become design values rather than placeholders.
3. Confirm the transverse-shear strength of the actual foam grade against its datasheet or an ASTM C273 test, since the computed core shear already exceeds the comparable published value at the placeholder pressure.
4. Obtain current local quotations for foam, glass, resin, and yard labour to convert the cost comparison into a firm break-even conclusion.

REFERENCES

Allen, H. G. (1969). Analysis and Design of Structural Sandwich Panels. Pergamon Press.

Belinha, J. (2024). Multiscale analysis of sandwich beams with polyurethane foam core: a comparative study of finite element methods and radial point interpolation method. Materials, 17(18), 4466.

Boesono, H., Saraswati, M., & Setiyanto, I. (2018). Analisis penggunaan foam polyurethane pada kapal ikan 5 GT sebagai daya apung cadangan. Saintek Perikanan (IJFST), 13(2), 82–88.

Eashwar Raaj, K., Naveen, J., Karthikeyan, N., Khan, T., & Sebaey, T. A. (2024). Effect of cellulose nanocrystals on the mechanical and free vibration behavior of hybrid glass/kenaf fiber reinforced polyurethane core-based sandwich structures. Journal of Natural Fibers.

Febrian, S., & Buwono, A. (2024). Fiberglass construction testing simulation on boat hulls. Jurnal Sains & Teknologi, Universitas Darma Persada, 14(1).

General Plastics Manufacturing Company. (2022). LAST-A-FOAM FR-3700 — Technical data and ASTM C273 shear properties. Tacoma, WA.

Gibson, L. J., & Ashby, M. F. (1997). Cellular Solids: Structure and Properties (2nd ed.). Cambridge University Press.

Hamilton, A. R., Thomsen, O. T., Madaleno, L. A. O., Jensen, L. R., Rauhe, J. C. M., & Pyrz, R. (2013). Evaluation of the anisotropic mechanical properties of reinforced polyurethane foams. Composites Science and Technology, 87, 210–217. https://doi.org/10.1016/j.compscitech.2013.08.013

International Organization for Standardization. (2019). ISO 12215-5:2019 Small craft — Hull construction and scantlings — Part 5: Design pressures for monohulls, design stresses, scantlings determination. ISO.

Junaedi, H., Khan, T., & Sebaey, T. A. (2023). Characteristics of carbon-fiber-reinforced polymer face sheet and glass-fiber-reinforced rigid polyurethane foam sandwich structures under flexural and compression tests. Materials, 16(14), 5101.

Jurnal Jaring SainTek. (2022). Studi Kekuatan Impact Laminasi Sistem Sisip (Sandwich) Fiberglass dan Polyurethane Foam. Universitas Bhayangkara Jakarta Raya.

Kim, M.-S., Kim, J.-H., Kim, S.-K., & Lee, J.-M. (2019). Effect of repetitive impacts on the mechanical behavior of glass fiber-reinforced polyurethane foam. Journal of Ocean Engineering and Technology, 33(1).

Logan, D. L. (2017). A First Course in the Finite Element Method (6th ed.). Cengage Learning.

Mohd Radzi, F. S., Abu Bakar, A., Asyraf, M. A., Nik Abdullah, N. A., & Suriani, M. J. (2022). Manufacturing defects and interfacial adhesion of Arenga Pinnata and kenaf fibre reinforced fibreglass/kevlar hybrid composite in boat construction application. Physical Sciences Reviews.

Quang, et al. (2025). Using modified castor oil as bio-polyol in preparation of water-blown rigid polyurethane foam with microcrystalline cellulose reinforcement. ChemistrySelect, 10.

Rathika, M., Mahesh Kumar, M., Paul Vizhian, S., Gangadhar Shetty, B., & Krishna, M. (2024). The effect of damages on modal frequencies of flat glass fiber reinforced polyurethane foam sandwich structures. Journal of Physics: Conference Series, 2748(1), 012010.

Shivakumar, N. D., & Deb, A. (2022). Dependence of the mechanical properties of rigid PU foam on density. Journal of Reinforced Plastics and Composites, 41(9–10).

Timoshenko, S. P., & Woinowsky-Krieger, S. (1959). Theory of Plates and Shells (2nd ed.). McGraw-Hill.

Wang, S., Tan, L., Yang, Z., Zhao, H., & Guo, L. (2024). A strong, tough, and stable composite with nacre-inspired sandwich structure. Advanced Materials, 36.

APPENDIX

APPENDIX 1 RIGID POLYURETHANE FOAM (RPUF)

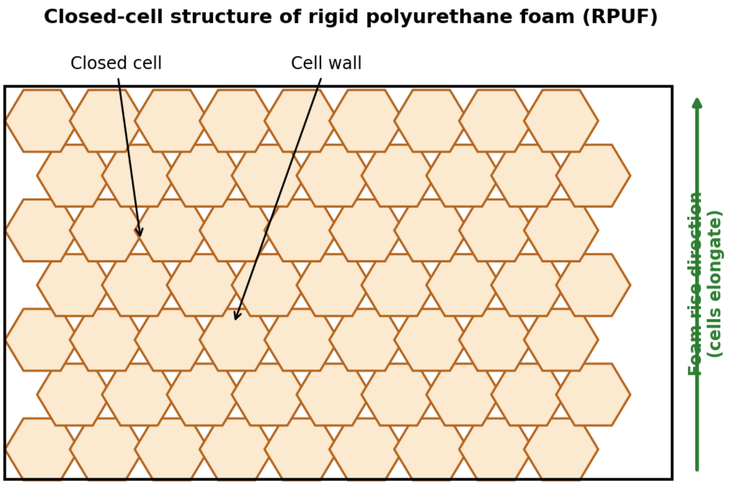

Figure A.1 Closed-cell structure of rigid polyurethane foam (RPUF).

Rigid closed-cell polyurethane foam (RPUF) is the core material analysed in this study. It is formed by reacting a polyol with an isocyanate; gas generated during the reaction expands the mixture into a closed-cell cellular solid whose density can be controlled over a wide range. Because the cells elongate along the direction in which the foam rises during curing, the cured foam is orthotropic (transversely isotropic): it is stiffer and stronger parallel to the rise direction ($\sigma\|$) than perpendicular to it ($\sigma\perp$).

The mechanical properties scale strongly with density. Following the Gibson–Ashby relations for closed-cell foam, the modulus scales approximately with the square of relative density and the strength with relative density to the power 1.5. The orthotropic elastic constants used in this study (Chapter 4) span the producible range of 40–120 kg/m³.

Representative shear properties for marine-grade rigid PU foam are given by the LAST-A-FOAM FR-3700 series (General Plastics, ASTM C273): the shear strength rises from about 280 kPa at 48 kg/m³ to about 1150 kPa at 128 kg/m³, with the 80 kg/m³ grade giving about 620 kPa. These values set the allowable used to check the sandwich core shear in Chapter 5.

Typical marine uses of RPUF include sandwich-panel cores, reserve-buoyancy filling, and thermal insulation.

APPENDIX 2 FIBERGLASS (E-GLASS/EPOXY LAMINATE)

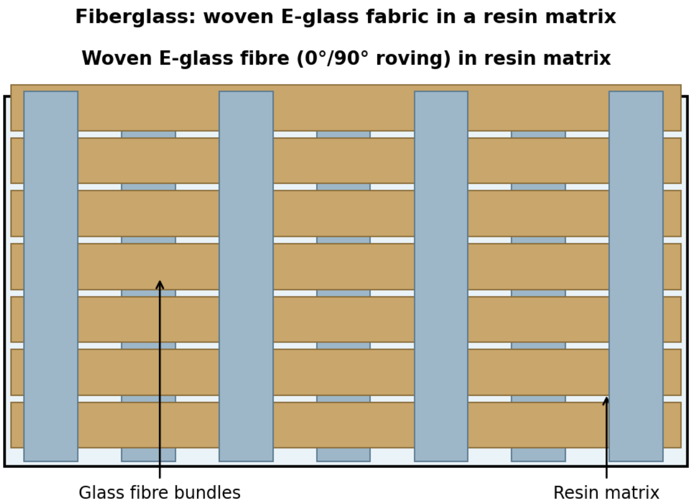

Figure A.2 Woven E-glass fibre fabric in a resin matrix (fiberglass).

Fiberglass, or fiber-reinforced plastic (FRP), forms the face sheets (skins) of the sandwich panel analysed in Chapter 5. It consists of E-glass fibres embedded in a thermosetting resin (epoxy in this study). The fibres carry the in-plane tensile and compressive loads while the resin transfers load between fibres and holds the laminate together. Woven-roving E-glass/epoxy with a balanced 0/90 architecture is the common marine skin laminate.

The skins are modelled as a homogenised orthotropic solid with representative properties: in-plane modulus about 16 GPa, through-thickness modulus about 7 GPa, in-plane shear modulus about 3.5 GPa, in-plane Poisson's ratio about 0.15, and density about 1800 kg/m^3 at roughly 50% fibre volume fraction. For thesis-quality results these constants should be replaced by the yard's actual laminate schedule, obtained from the supplier datasheet, classical lamination theory applied to the real ply schedule, or a coupon tension test.

Fiberglass is favoured in marine construction for its high strength-to-weight ratio, corrosion resistance, formability into complex hull shapes, and low maintenance compared with wood or metal.

This page has been intentionally left blank.

AUTHOR BIOGRAPHY

Gilang Gemilang Wahyu Wahab, that is the full name of the Author. Born in Medan on Maret 1, 2005, the Author is the second child in the family. The Author completed formal basic education at Medan International School, then continued to SMP Harapan 1, and SMAN 1 Kota Medan. After graduating from high school, the Author was accepted into the Department of Naval Architecture at FTK ITS in 2022 through Independent admition selection.

In the Department of Naval Architecture, the Author is pursuing the Field of Study in Naval Architecture. The Author has also participated in the PKM at the ITS level and several other scientific writings.

Email: gilanggemilangww27@gmail.com